2004-03

Acoustic properties of toroidal bubbles and construction of a large apparatus

Harris, Ashley M.

Monterey, California. Naval Postgraduate School

NAVAL POSTGRADUATE SCHOOL

MONTEREY, CALIFORNIA

THESIS

ACCOUSTIC PROPERTIES OF TOROIDAL BUBBLES AND CONSTRUCTION OF A LARGE APPARATUS

by

Ashley M. Harris

March 2004

Thesis Advisor:	Bruce C. Denardo
Second Reader:	Ronald Brown

THIS PAGE INTENTIONALLY LEFT BLANK

REPORT DOCUMENTATION PAGE		Form Approved OMB No. 0704-0188

1. AGENCY USE ONLY *(Leave blank)*	2. REPORT DATE	3. REPORT TYPE AND DATES COVERED
	March 2004	Master's Thesis

4. TITLE AND SUBTITLE: Acoustic Properties of Toroidal Bubbles and Construction of a Large Apparatus	5. FUNDING NUMBERS
6. AUTHOR(S) Ashley M. Harris	
7. PERFORMING ORGANIZATION NAME(S) AND ADDRESS(ES) Naval Postgraduate School Monterey, CA 93943-5000	8. PERFORMING ORGANIZATION REPORT NUMBER
9. SPONSORING /MONITORING AGENCY NAME(S) AND ADDRESS(ES) N/A	10. SPONSORING/MONITORING AGENCY REPORT NUMBER

11. SUPPLEMENTARY NOTES The views expressed in this thesis are those of the author and do not reflect the official policy or position of the Department of Defense or the U.S. Government.

12a. DISTRIBUTION / AVAILABILITY STATEMENT	12b. DISTRIBUTION CODE
Approved for public release; distribution is unlimited	A

13. ABSTRACT (maximum 200 words)

When a burst of air is produced in water, the result can be a toroidal bubble. This thesis is concerned with experimental investigations of three acoustical properties of toroidal bubbles: (i) propagation through high-intensity noise, (ii) emission, and (iii) scattering. In (i), an attempt to observe a recent prediction of the acoustic drag on a bubble is described, which is analogous to the Einstein-Hopf effect for an oscillating electric dipole in a fluctuating electromagnetic field. No effect was observed, which may be due to insufficient amplitude of the noise. In (ii), observations of acoustic emissions of volume oscillations of toroidal bubbles are reported. Surprisingly, the emission occurs primarily during the formation of a bubble, and is weak in the case of very smooth toroidal bubbles. In (iii), we describe an experiment to observe the effect of a toroidal bubble on an incident sound field. In addition to the acoustical investigations, we describe the construction of a large hallway apparatus for further investigations and for hands-on use by the public. The tank has cross section 2 feet by 2 feet and height 6 feet, and the parameters of reservoir pressure and time between air bursts are adjustable by the observer.

14. SUBJECT TERMS Toroidal Bubble, Acoustic Emission, Vortex Ring	15. NUMBER OF PAGES 77
	16. PRICE CODE

17. SECURITY CLASSIFICATION OF REPORT	18. SECURITY CLASSIFICATION OF THIS PAGE	19. SECURITY CLASSIFICATION OF ABSTRACT	20. LIMITATION OF ABSTRACT
Unclassified	Unclassified	Unclassified	UL

NSN 7540-01-280-5500

Standard Form 298 (Rev. 2-89)
Prescribed by ANSI Std. 239-18

THIS PAGE INTENTIONALLY LEFT BLANK

Approved for public release; distribution is unlimited

ACOUSTIC PROPERTIES OF TOROIDAL BUBBLES AND CONSTRUCTION OF A LARGE APPARATUS

Ashley M. Harris
Lieutenant, United States Navy
B.S., United States Naval Academy, 1997

Submitted in partial fulfillment of the
requirements for the degree of

MASTER OF SCIENCE IN APPLIED PHYSICS

from the

NAVAL POSTGRADUATE SCHOOL
March 2004

Author:

Ashley M. Harris

Approved by:

Bruce C. Denardo, Thesis Advisor

Ronald Brown, Second Reader

James H. Luscombe
Chairman, Department of Physics

THIS PAGE INTENTIONALLY LEFT BLANK

ABSTRACT

When a burst of air is produced in water, the result can be a toroidal bubble. This thesis is concerned with experimental investigations of three acoustical properties of toroidal bubbles: (i) propagation through high-intensity noise, (ii) emission, and (iii) scattering. In (i), an attempt to observe a recent prediction of the acoustic drag on a bubble is described, which is analogous to the Einstein-Hopf effect for an oscillating electric dipole in a fluctuating electromagnetic field. No effect was observed, which may be due to insufficient amplitude of the noise. In (ii), observations of acoustic emissions of volume oscillations of toroidal bubbles are reported. Surprisingly, the emission occurs primarily during the formation of a bubble, and is weak in the case of very smooth toroidal bubbles. In (iii), we describe an experiment to observe the effect of a toroidal bubble on an incident sound field. In addition to the acoustical investigations, we describe the construction of a large hallway apparatus for further investigations and for hands-on use by the public. The tank has cross section 2 feet by 2 feet and height 6 feet, and the parameters of reservoir pressure and time between air bursts are adjustable by the observer.

THIS PAGE INTENTIONALLY LEFT BLANK

TABLE OF CONTENTS

THIS PAGE INTENTIONALLY LEFT BLANK

LIST OF FIGURES

THIS PAGE INTENTIONALLY LEFT BLANK

LIST OF TABLES

THIS PAGE INTENTIONALLY LEFT BLANK

ACKNOWLEDGMENTS

My work here at the Naval Postgraduate School is dedicated to my mother and father, Wanda and Kenneth Harris without whose love and support I would not be here today. My father is a Navy veteran who inspired me to join the Navy.

Professor Bruce Denardo, my thesis advisor, whose passion for physics initially excited me about this project. His is endless knowledge and energy were critically important to the completion of this work. I thank him for his help, guidance and most importantly his patience,

George Jaksha for all of his input for the underwater and large apparatus. His detailed construction knowledge ,experience and skill were instrumental in producing designs which functioned as intended. Also, he shares my passion for classic cars and we have had numerous conversations about my projects which didn't just involve physics.

THIS PAGE INTENTIONALLY LEFT BLANK

I. INTRODUCTION

When a burst of air is produced in water, the resultant bubble can form a toroid similar to a vortex or smoke ring. It is remarkable that such a smooth ordered structure can arise from a highly turbulent burst of air in water. Some dolphins generate an impressive variety of toroidal bubbles, apparently for entertainment. Small toroidal bubbles can occur in the cavitation collapse of spherical bubbles near a solid surface, which can damage propeller blades (Blake,1999) (Sussman,1997) and cause acoustic emission. Large toroidal bubbles have been proposed as an anti-torpedo defense for submarines. However, few experiments are in the scientific literature. In the past, NPS thesis student Allen Hobbs built an apparatus to generate and observe large toroidal bubbles, and quantified the conditions for which toroidal bubbles occur (Hobbs, 2000). The purpose of the current thesis is to explore various acoustic properties of toroidal bubbles, and to initiate the construction of a large apparatus that will serve both as a system with which future data will be taken and as a hallway apparatus for the public.

Vortex motion of fluids is readily observed and demonstrated, and has fascinated people for many centuries, as evidenced by stories of giant whirlpools that have swallowed ships. Descartes originated a theory in which vortices were responsible for planetary motion. Extensive analytical development of vortices occurred in the second half of the 1800's due to Helmholtz, Kelvin, J. J. Thompson, and others (Lamb,1997). Kelvin proposed a theory of atoms based on vortex rings in the ether (Acheson,1990). A recent example of vortex motion is the observation of "dust devils" (small tornadoes) on the surface of Mars (Metzer,2000). Pairs of dust devils have been observed, which typically have oppositely directed circulations, causing a pair to translate rather than rotate. In super fluid ^{4}He, quantized vortex lines and rings can occur, (Putterman,1974) (Reif,1964) (Faber,1995) and elementary excitations referred to as *rotons* may

be microscopic vortex rings (Faber,1974). Quantized vortices in a stirred Bose-Einstein condensate have recently been observed (Fitzgerald,2000).

A toroidal vortex ring is a vortex ring whose core consists of a different fluid than the surrounding fluid. A standard vortex ring is the limiting case in which the two fluids are the same. This can be demonstrated in the case of a "smoke ring" with a large cardboard box with a roughly four-inch diameter hole cut at the center of the front face. The cardboard is removed from the back face, which is covered with a thin plastic sheet that is taped to the box. The back is tapped to produce vortex rings, which can be evidenced by their effect on lightweight ribbons or a person with long flexible hair. Smoke from a fog machine is then fed into the box, and the back is again tapped by hand. This produces a dramatic visualization of the vortex rings. The smoke is drawn to the region near the core by the lower pressure according to Bernoulli's law. (In the core, the flow is rotational and Bernoulli's law does not apply.) The flow of a vortex ring can be demonstrated by having it extinguish a distant candle flame. It should be noted that performing the demonstrations in this manner shows that the smoke only serves to visualize the rings. Standard vortex rings can also be demonstrated by allowing drops of colored water to strike the surface of a container of water (Batchelor,1967), and experiments have been conducted on such drop-generated vortex rings (Shankar,1995). Toroidal vortex rings can be demonstrated by employing a dissimilar liquid (for example, Pepto Bismal™ or colored salt water (Reif,1964) as the drops. The mushroom effect of explosions motivated an early investigation of toroidal vortex rings (Turner,1957). The heat due to the explosion causes the air that is convected by the vortex ring to have less density than the surrounding air. A motivation of this investigation was the possibility of employing vortex rings to seed clouds in order to produce rain.

A toroidal bubble is a special case of a toroidal vortex ring in a liquid where the core is gaseous. Although there is a significant amount of analytical (Turner,1957) (Pedley,1968) (Lundgren,1991) and numerical (Lundgren,1991) (Chen,1999) (Sussman,1997) work related to large toroidal bubbles, there are apparently only two experimental investigations, (Walters,1963) (Turner,1957).

In Ch. II, we discuss an experiment in which toroidal bubbles travel through high-intensity acoustic noise. We were motivated to perform this experiment due to the theoretical work of Larraza and Tucholski (2000), who showed that noise causes an additional drag on a spherical bubble. Surprisingly, this drag is predicted to be negative (i.e., a positive driving force) under certain conditions.

In Ch. III, we discuss experiments in which we measure the acoustic emission and absorption of toroidal bubbles. Whether or not a toroidal bubble forms is a highly stochastic process. That is, for the same parameters, a toroid may form one time but not another, which is not surprising due to the very turbulent nature of the initial burst of gas. One of our motivations for examining acoustic emissions was to try to observe a signature that allows prediction of whether or not a toroidal bubble would form. This would be analogous to tornado prediction, and may offer some insight into this important problem.

In Ch. IV, we describe our initial construction of a large apparatus for the production of toroidal bubbles. The apparatus will serve two purposes. First, a variety of investigations can be pursued with a large apparatus. Photographing a sequence of the formation of a toroidal bubble would be useful in order to understand the process. The speed of a toroidal bubble decreases and the ring diameter increases as the toroid rises. Data on this evolution can be gathered and analyzed. Another aspect is to understand the instability that eventually occurs when a toroid breaks into many spherical bubbles. The second purpose of the large apparatus is for hands-on use by the public. The apparatus will be placed in the hallway of the first floor of Spanagel Hall. The Exploratorium (San Francisco, California) had a toroidal bubble display in the late 1980's, but the apparatus was not hands-on and is only very briefly described in the literature (Semper,1992). There is now a new toroidal bubble exhibit in which the bubbles are created by the observer with a hand pump. As described in Ch. IV, our apparatus is much more versatile.

THIS PAGE INTENTIONALLY LEFT BLANK

II. PROPAGATION THROUGH ACOUSTIC NOISE

In this chapter, we consider the motion of toroidal bubbles through high-intensity broadband acoustic noise. According to recent theoretical results by Larraza and Tucholski (2000) as explained in Sec. II.A, we expect toroidal bubbles to move more slowly due to the presence of noise. The final acoustic set-up for the experiment is described in Sec.IIC, and the results are presented in Sec. IID.

A. ACOUSTIC DRAG

Larraza and Tucholski (2000) have shown theoretically that spherical bubbles in a uniform broadband acoustic noise field experience a drag force due to the noise. The effect is analogous to the Einstein-Hopf drag on an oscillating electric dipole in a thermally fluctuating electromagnetic field. For an acoustic noise spectrum whose spectral energy density ε is independent of frequency, the force on a bubble is

$$\mathbf{F} = -\pi^2 a \varepsilon \mathbf{v} \qquad \text{(II.A.1)}$$

where a is the ambient radius of the bubble, **v** is the velocity of the bubble, and ε has units of energy per volume per frequency. The result is valid for a uniform band-limited spectrum if the resonance frequency of spherical volume oscillations of the bubble lies within the uniform region of the band. For a non-uniform noise spectrum, Larraza and Tucholski showed that the expression (II.A.1) is modified in two ways: ε is evaluated at the resonance frequency of the bubble, and there is an additional term proportional to the derivative of the energy density with respect to frequency, also evaluated at the resonance frequency. Remarkably, because this derivative can be positive or negative with arbitrarily large magnitude, it is possible for the noise to cause the bubble to have *positive*

acceleration ("negative drag"). The noise would thus cause the terminal velocity to be greater.

The corresponding theory for toroidal bubbles in an acoustic noise field has not yet been done, but these bubbles are expected to behave similarly as spherical bubbles. The drag may be more apparent for toroidal bubbles due to a possibly greater quality factor of the volume oscillation mode. We were thus motivated to perform an experiment to observe a significant slowing of the motion of toroidal bubbles in an acoustic noise field. We focus only on the effect represented by Eq. (II.A.1) for broadband noise, because toroidal bubbles are produced with randomly varying shapes, and because these bubbles change shape and thus resonance frequency as they propagate. It would thus be very difficult to observe the negative drag effect which is predicted to arise when the noise spectrum is a strongly varying function of frequency near the bubble resonance frequency.

The resonance frequency of volume oscillations of a spherical bubble is (Kinsler et al., 2000)

$$f_o = \frac{1}{2\pi a}\sqrt{\frac{3\gamma p_b}{\rho_o}}\ , \qquad \text{(II.A.2)}$$

where a is the radius of the bubble (as above), γ is the ratio of specific heats of the gas, p_b is the pressure inside the bubble, and ρ_o is the density of the liquid. Equation (II.A.2) can be used to obtain a rough value of the resonance frequency of toroidal bubbles. For a = 0.5 cm, γ = 1.4, $p_b = p_o = 1.0 \times 10^5$ N (atmospheric pressure), and $\rho_o = 1.0 \times 10^3$ kg/m^3, the resonance frequency is f_o = 650 Hz. In our experiments, we accordingly choose the band of the noise to be 250 Hz to 1.0 kHz.

B. APPARATUS

The toroidal bubble apparatus of Hobbs (2000) was adapted for our experiments on the propagation of toroidal bubbles through acoustic noise. A diagram of the apparatus is shown in figure II.B.1. This apparatus was convenient not only because it already existed, but also because it was well quantified. In particular, we utilized Hobbs' extensive search of solenoids, nozzles, and drive parameter values (reservoir pressure, on-time of the electrical pulse to the solenoid, and minimum repeat time) that yield smooth toroidal bubbles most frequently. This is important because the formation of toroidal bubbles is a highly stochastic process even for optimum conditions.

This acoustic experiment calls for the production of acoustic noise in a range which could possibly excite modes of the bubble. In order to conduct our acoustic trials we added several pieces of equipment to the existing apparatus. Adding a transducer requires the use of a power amplifier, a function generator and a band-pass filter. A separate omni-directional hydrophone is required to take measurements of the acoustic field produced by the transducer and the use of the hydrophone requires the addition of a preamplifier.

The amplifier that was added to the apparatus is a dual-channel output professional stereo amplifier model MX 3000a manufactured by QSC Audio . Each separate channel has it own power transformer and bipolar power supply. Also built into each channel are special clip-limiting circuitry and overload protection as a safety precaution to prevent any possible damage to a transducer or speaker. This power amplifier is capable of operating in a bridged mode with a maximum voltage gain of 38 dB and a maximum power output of 3.2 kW. The low-noise preamplifier added is model SR560 manufactured by Stanford Research Systems. It provides low-noise amplification of single-ended and true differential input signals at gains of 1 to 50,000. This amplifier was used in conjunction with an omni-directional hydrophone for all acoustic measurements. This mid-frequency hydrophone model ITC-1032, manufactured by International

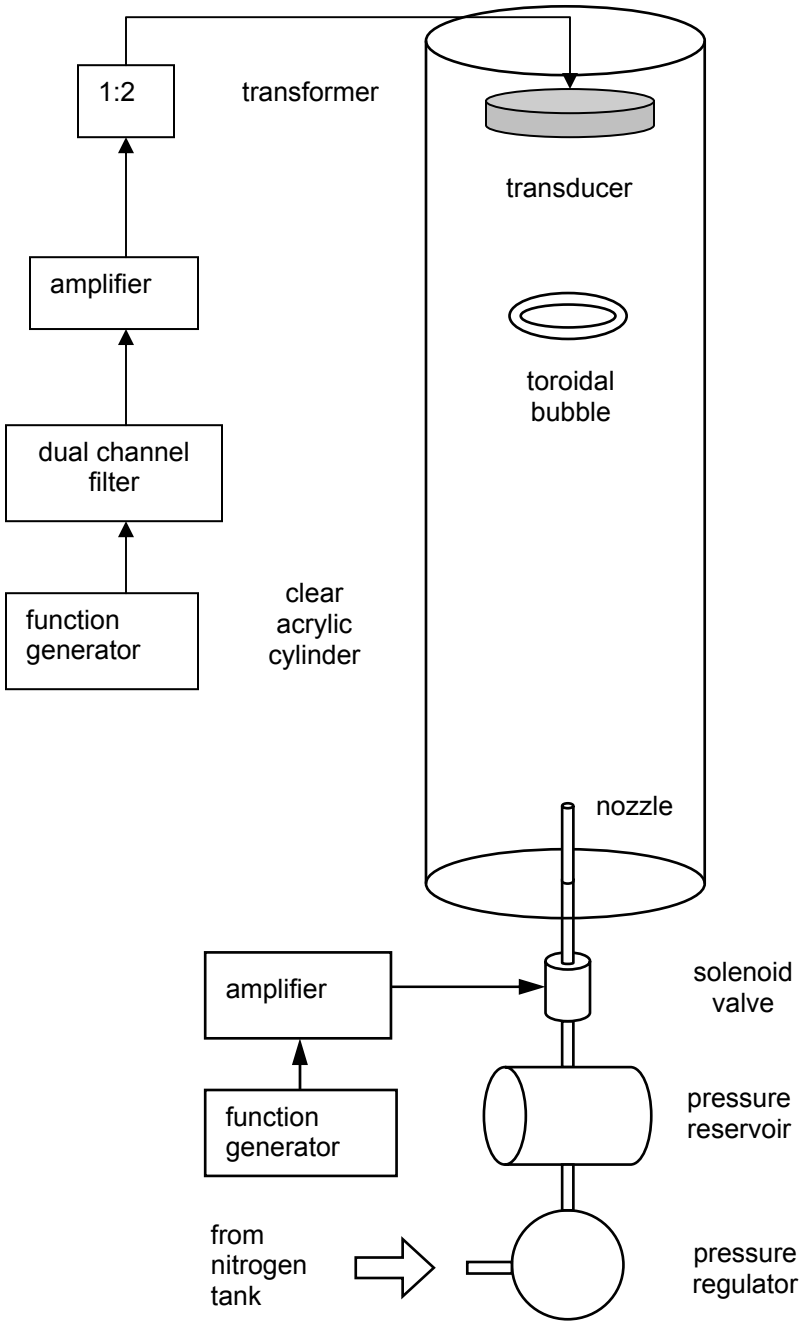

Figure II.B.1. Diagram of the apparatus of Hobbs (2000) used to investigate the formation of toroidal bubbles and the equipment we added to power the acoustic transducers. The acrylic cylinder is 4 feet in height and 1 foot in diameter. We employed this apparatus for an investigation of the propagation of toroidal bubbles through high-intensity acoustic noise.

Transducer Corporation, has a resonant frequency of 31 kHz. It is piezoelectric spherical shell with a diameter of 70 mm. Overall length including the bonded shielded cable assembly connection is 16.5 cm.

To power the acoustic transducer, several additional pieces of electronics were also added. The source of the noise signal is an HP33120A function generator in the noise mode with the peak to peak voltage at the maximum setting of 10 V. At this noise setting on the HP33120A generates noise in a band from 100 Hz to 250 kHz. The SR640 dual-channel filter is a combination high-pass/low-pass filter with built in preamplifier manufactured by Stanford Research Systems. A band pass filter is required to achieve the desired noise band for the experiment. We set the high-pass filter at 250 Hz and the low-pass filter at 1.0 kHz. In order to maximize the voltage received by the transducer/driver as a way to further increase the acoustic intensity in the tank we added a 1:2 step up transformer. This voltage transformer is a generic off-the-shelf type for 120 V to 240 V conversion. A schematic of the transducer apparatus is shown in figure II.B.1.

C. PRELIMINARY TRIALS

The initial limiting factors in choosing a laboratory set-up for the acoustical noise propagation experiments were the size of the apparatus tank and the possible interference in the rising run of the bubble by the transducer and/or wiring to the transducer. The small size of the apparatus (1 ft diameter) was very limiting to the type of transducers which could be successfully employed for the experiment. To ensonify the water in the tank, we were advised that the typical piezoelectric transducers that are used in underwater sound generation would not be effective at the low frequencies of interest (250 Hz to 1.0 kHz), and that we should employ a high-intensity compression driver in air near the top of the tank. Such a driver in the required frequency range is the JBL 2490. Although this driver is not common, there were several new ones in the laboratory. It was decided to make an initial test using an acoustic compression driver and make

comparisons to available transducers which are small enough to provide the least possible interference. Acoustic pressure in the tank was measured with an ITC-1032 hydrophone, which was subsequently used for all acoustic measurements. An acoustic compression driver mounted over the top of the apparatus tank would be the best possible solution if it produced high intensity sound in the water column as it would eliminate any possible interference with rise time of the bubble.

The compression driver was mounted above the water tank using 4-3/8-inch 6 inch long bolts threaded into the mounting holes which are spaced 90º apart on the face of the driver. A lattice of rod was assembled using table clamps to position three vertical 2 meter rods around the tank. Two horizontal rods were mounted to the vertical rods in order to create a platform to which the mounting bolts could be clamped. The final position of the driver was 6 inches above the surface of the water and centered in the tank. The mounting bolt heads were above the top of the tank so that the tank could be covered when not in use, which inhibits calcium deposition on the tank wall at the water line due to evaporation. If the driver was eventually used for the experiment, we planned to hacksaw the bolts so that the driver would be nearer the surface of the water. The JBL compression driver and the mounting assembly are shown in figure II.C.1.

Using the HP 33120A function generator and the QSC MX3000 amplifier, 20 V was applied to the compression driver at both 250 Hz and for a noise band from 250 Hz and 1.0 Hz. The maximum received voltage using the ITC-1032 transducer was 1.2 V using 10 dB gain on the SR560 pre-amplifier. Though there can be no interference with the bubble a negative effect of using a compression driver was the extremely high sound level produced in the laboratory. Double hearing protection was required for anyone in the laboratory while the driver was operated at maximum power.

A trial was then conducted using an ITC-5117 acoustic transducer. This type of transducer is not ideal for the frequency ranges which are required as they are designed for use as depth sounders and fish finders. The transducer

Figure II.C.1. Mounting of a high-intensity air compression driver (JBL 2490) above the toroidal bubble tank. The diameter of the tank is 1 foot.

has length 5.0 inches and diameter 2.57 inches. The resonance frequency is 120 kHz with a conical beam pattern which is 14 degrees wide at the 3 dB points.

Using the function generator and the power amplifier with a 1:2 transformer, 370 V was applied to the transducer at both 250 Hz and for noise in the band from 250 Hz and 1.0 kHz. The maximum received voltage using the ITC-1032 transducer was 0.66 V, where the SR560 pre-amplifier was set with no gain. This was a sound pressure level that was roughly an order of magnitude greater than that delivered by the compression driver. This result showed us that the best results would be achieved by using an underwater acoustic transducer, especially because the ITC-5117 model is far from ideal.

A trial was then conducted using an ITC-5095 acoustic transducer. This type of transducer is designed for use as depth sounders and fish finders as the previous model. The dimensions of are the same as the ITC-5117. The resonance frequency is 100 kHz which was slightly lower than the ITC-5117 with the same conical beam pattern which is 14 degrees wide at the 3 db points. Using the same set-up as the previous transducer, we found that the maximum received voltage of the ITC-1032 transducer was 0.65 V with 0 dB gain on the SR560 pre-amplifier. This result was virtually the same as reached with the ITC-5117 model.

A final trial was then conducted using a dual tri-laminar flexural disk. This transducer was designed and built by LT Toby Lemerande as a student project for Dr. Hofler's PH4454 Transducer Theory and Design class at the Naval Post Graduate School (Lemerande,2001) . The resonance frequency of the unit is 1.4 kHz. Using the same set-up from the previous cases, 360 V was applied to the flexural disk transducer (FDT) at both 250 Hz and with noise in the band between 250 Hz and 1.0 kHz. The maximum received voltage at the pure tone was 1.20 V with 0 dB gain on the SR560 pre-amplifier. It was observed that when more than 270 V was applied with the pure tone, the acoustic pressure produced was capable of triggering the solenoid valve into the open position. This problem was not encountered in the noise band-passed configuration. Based on the received voltage we concluded that the FDT produced the highest sound intensity in the water, and we thus used it for the experiment.

D. EXPERIMENTAL RESULTS

Upon selecting the best transducer, we began making the determination of the configuration which would provide the best experimental results. Because of the highly stochastic nature of toroidal bubble formation, we selected a solenoid activation time corresponding to a frequency of 70 Hz for the function generator and a reservoir pressure of 2.5 psi. Based on the prior work by Hobbs (2000),

these settings would provide the highest percentage of toroidal bubble formations per solenoid triggering.

The experiment was conducted by measuring the travel time of the bubble from the toroidal formation to the impact with the surface of the water at the top of the tank. Rise times were recorded for twenty toroidal bubbles in a noise free environment followed by twenty toroidal bubbles in band-passed noise generated by the HP33120A signal generator. This signal would be band-passed between 250 Hz and 1.0 kHz through the SRS650 band-pass filter. While gathering data times it is important to alternate between the noise and no-noise settings to verify that no changes have occurred in the toroidal bubble generation settings. If a negative change occurred during the noise run it would possibly become visually apparent. Also this allows for a statistical comparison as a further verification that there is no significant change in the toroidal formation regime over the time frame of data collection which could skew the results.

Another important consideration is the placement of the transducer in the tank. Ideally, the noise field generated would be uniform in the apparatus tank. Two FDT's were available but the resonance frequencies were substantially different (student projects) and several different configurations were tried: a single transducer at the bottom, a single transducer at the top, and two transducers, one at the top and the other at the bottom. Measurements were taken with the ITC-1032 hydrophone throughout the tank and the best results were achieved with a single FDT with the lowest resonance frequency either at the bottom or at the top. This is because we had only a single 3.0 kW amplifier and operating in the split channel mode reduced the power. An ideally uniform noise field could not be generated but the results achieved are approximately symmetrical about the middle, so the effect of the imbalance in radiation pressure should approximately cancel. Table II.D.1 shows the relative sound pressure level at various vertical locations in the tank.

Preliminary data with a single transducer resting on the bottom of the tank showed a significantly longer travel time for toroidal bubbles in the presence of acoustic noise. However, the rate of production of toroidal bubbles in the

presence of the noise was much less than the rate in the absence of noise. Furthermore, we had to limit the intensity of the noise because vibrations caused air to leak past the solenoid valve when the valve was closed. This could be inferred from bubbles that continually escaped from the nozzle. The reduced rate of production of toroidal bubbles, and the leaking past the valve, meant that the difference in travel times could be explained by the vibrations skewing the production of the bubbles in favor of slower-moving ones.

By moving the single transducer to the top of the tank, we found that the noise field was symmetrical with height and the vibration problem had been eliminated. Figure II.D.1 shows the final experimental configuration with the FDT placed at the top of the apparatus. From the calibration factor for the hydrophone, we determined that the average sound pressure level in the tank was 1.79×10^{9} μPa, or 185 dB for the standard water reference level of 1 μPa. The resultant data are shown in histograms in figure III.D.2. We measured the travel times of a total of 60 toroidal bubbles in the absence of noise, and 60 in the presence of noise. Visual inspection of the data shows no apparent difference in the distribution of times. This is confirmed by calculation of the mean and standard deviation of the mean for both cases when large times are rejected. These average travel times are (2.78 ± 54) seconds for no noise, and (2.75 ± 58) seconds for noise. Tables of the descriptive statistics for the data are shown in Appendix A.

We conclude that the noise has a negligible effect on the propagation of the toroidal bubbles. This is probably due to an insufficiently large sound pressure level of the noise. It is interesting that no difference in the times was observed. This indicates that that the effects of non-uniformity of the noise, and a possible skewness of toroidal bubble production due to the vibration of the valve and ensonification of the burst of gas, are negligible. Higher noise amplitudes may lead to these unwanted effects, but it is encouraging that they are absent at our noise amplitudes. Hence, the system remains a viable candidate for a future observation of acoustic-induced drag on bubbles.

Acoustic sound field in apparatus	
Tank Level	Received RMS Volts
Top (100 cm)	.42
¼ Top (75 cm)	.42
Middle (50cm)	.36
¼ Bottom (25 cm)	.40
Nozzle tip (0 cm)	.42

Table II.D.1: Hydrophone measurements at locations in the apparatus tank showing the approximate symmetrical nature of the sound field. The distance between the tip of the nozzle and the surface of the water is 120 cm.

Figure II.D.1. Apparatus for an experiment to measure the average velocity of toroidal bubbles in the presence of high-intensity acoustic noise. A transducer, which is partially submerged at the top of the tank, generates the acoustic field.

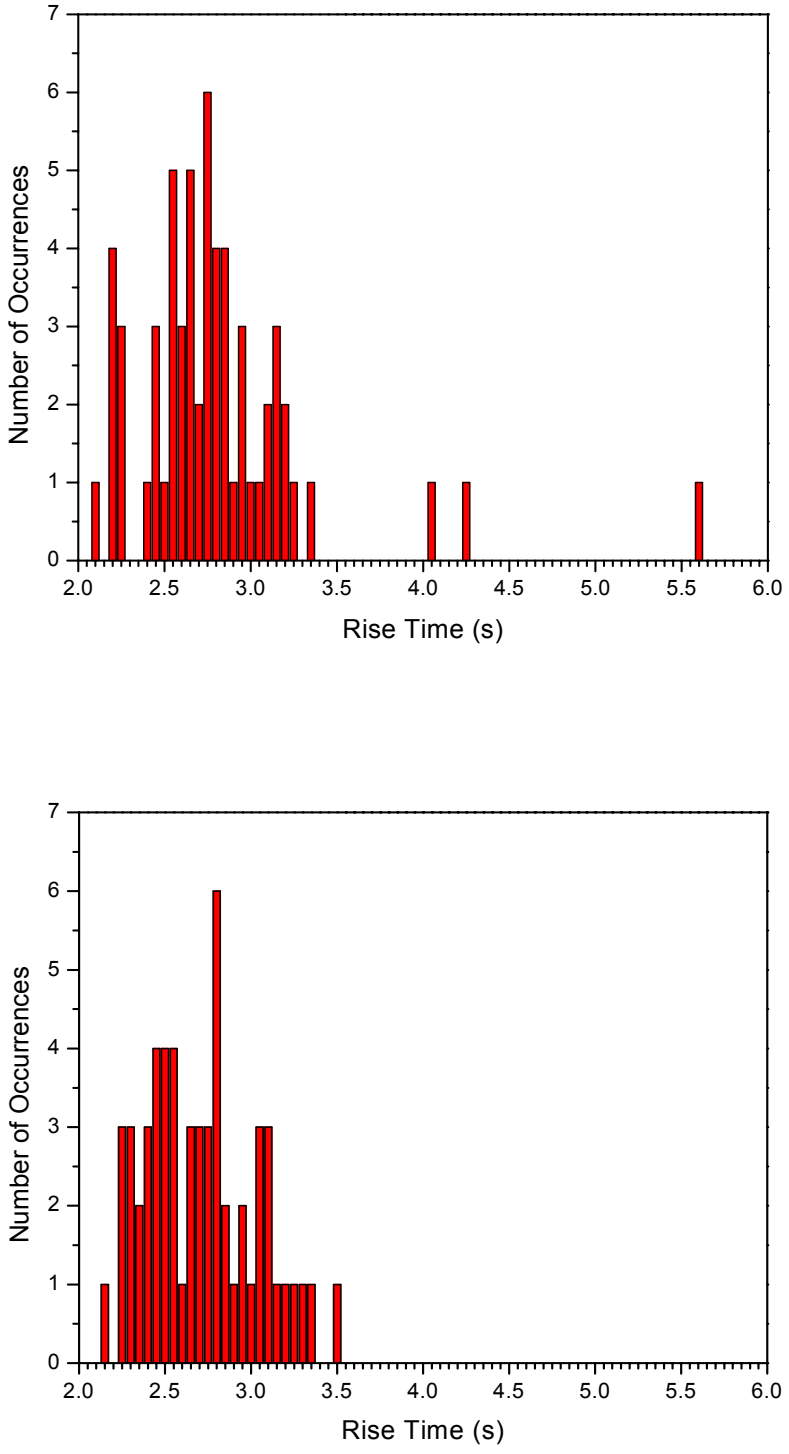

Figure II.D.2 Histograms of the bubble rise time. Top: 60 Bubbles with ambient noise only. Bottom: 60 Bubbles with added acoustic noise in the band from 250 Hz to 1.0

THIS PAGE INTENTIONALLY LEFT BLANK

III. ACOUSTIC EMISSION AND SCATTERING

The next stage of our research involves the acoustic emission and scattering toroidal bubbles. Of interest is whether or not the sound emitted by toroidal bubbles is detectable, and if so, whether a signal exists which could predict whether or not a toroidal bubble will form. In a preliminary investigation by Hobbs (2000), no signal was detected which could be distinctly assigned to a toroidal bubble. This measurement occurred in the small apparatus and it was assumed that the signal may have been obscured by the oscillations from the apparatus itself. To remove any possibility of interference due to the apparatus' acrylic walls and/or the solenoid valve we needed to generate toroidal bubbles in anechoic underwater environment. Modifying the existing apparatus was not feasible due to its size so we determined to make use of an existing anechoic tank with the inclusion of a new toroidal bubble apparatus.

A. UNDERWATER TOROIDAL BUBBLE APPARATUS

The available anechoic tank in the oceanography lab is large in size. It is 7.4 meters long, 2.0 m wide and 2.4 m deep with the side walls and bottom of the tank covered with anechoic tile or foam. By equating the length of the sidewall foam wedges to a quarter wavelength, it can be estimated that the anechoic effectiveness begins to decline at 10 kHz. The bottom is covered with anechoic tile with unknown properties but are assumed to be similar to the foam side walls. The tank is constructed into the floor of the basement and it has no access points from underneath. Any toroidal bubble apparatus would have to be lowered into the tank from the surface.

In designing a new apparatus we wanted it to operate in the same manner which had been developed by Hobbs. This operation, as described in sec.II.A, uses an electrically operated solenoid valve to release a burst of compressed nitrogen from a charged reservoir through a specially shaped nozzle which creates a toroidal bubble in the water. Unfortunately, the available electrically

operated solenoid valves are not waterproof and would require protection for underwater operation. Another element to consider in the design of the apparatus is maximizing the rise time of the bubble. The rise time is a function of the distance between the nozzle tip of the apparatus and the surface of the water. The apparatus size, specifically the height, would impact the rise time so a design which minimized apparatus height has higher desirability.

Our solution to all these requirements was an apparatus design in which the nitrogen reservoir would also act as the protective housing for the electronically operated solenoid valve. The preliminary concept design is seen in figures III.A.1 and III.A.2. The reservoir chamber is constructed out of 8 inch diameter PVC pipe mounted into 1 inch thick PVC plate. PVC was chosen as the base material for several reasons: reduced cost, availability and ease of construction. The lid is designed and built to be removable as a complete assembly secured by six 3/8-inch diameter bolts. This feature was added to make any change in the solenoid or inspection of the reservoir chamber fast for the operator.

These mounting bolts screw into a mounting ring which is added to the top of the PVC pipe. The mounting ring, also made of PVC, was machined to high tolerance and glued to the top of the reservoir. The high tolerance machining allowed for the use of standard glues and would greatly reduce the chance of leaks. As protection against wear, 3/8-inch nuts were machined and pressed into the ring instead of just threading the PVC directly. In order to provide increased waterproofing in the lid interface a groove was cut in the mounting ring to house a rubber o-ring.

The lid assembly is made from 1 inch thick PVC plate. The assembly includes the lid plate, the solenoid valve and the nozzle assembly. The solenoid valve is mounted in the lid with a threaded screw type fitting and can easily be unscrewed if a replacement is required. The nozzle assembly is mounted to a

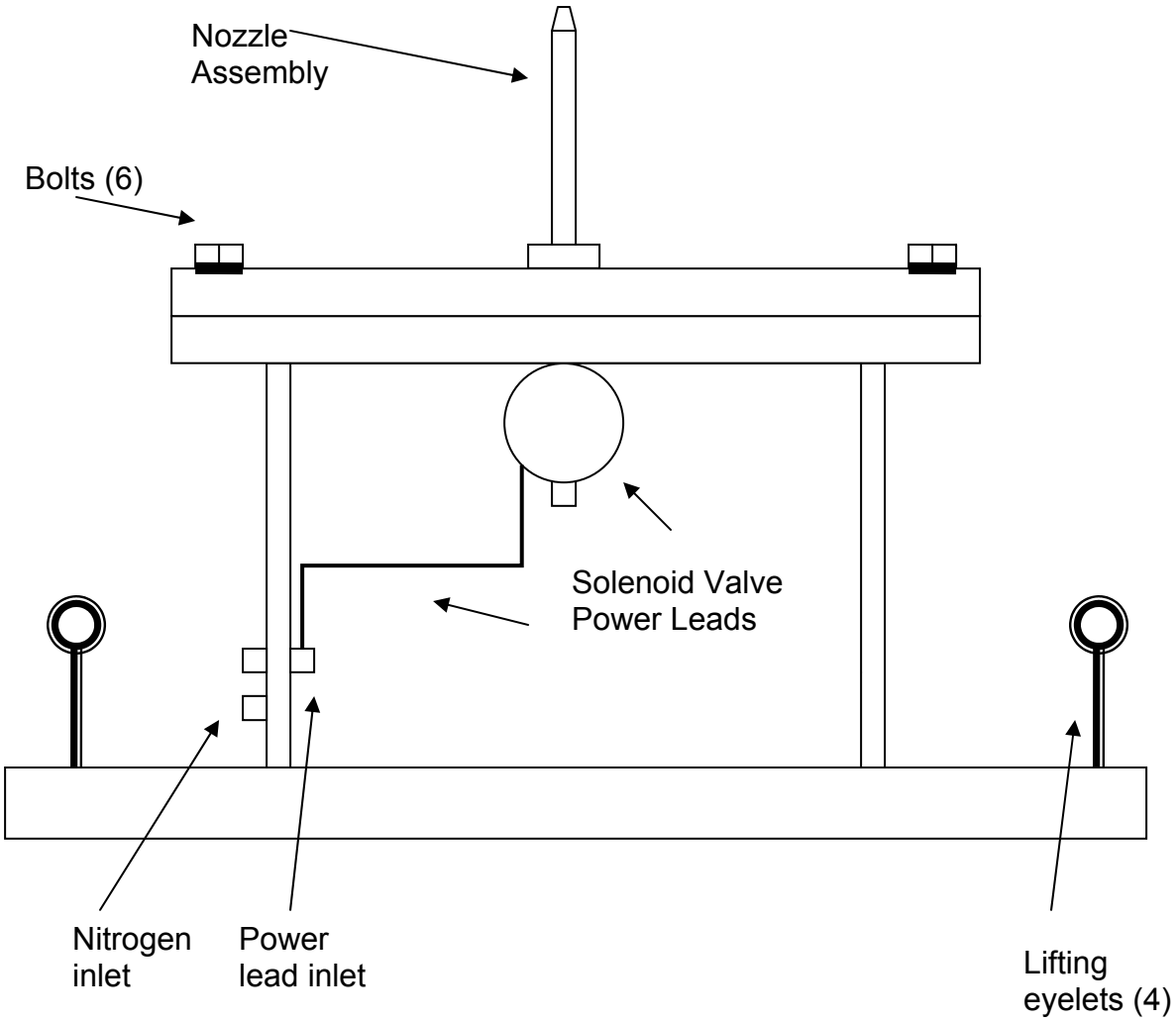

Figure III.A.1. Diagram showing a side cutaway view of the underwater toroidal bubble generator for use in the anechoic tank. (Not to scale)

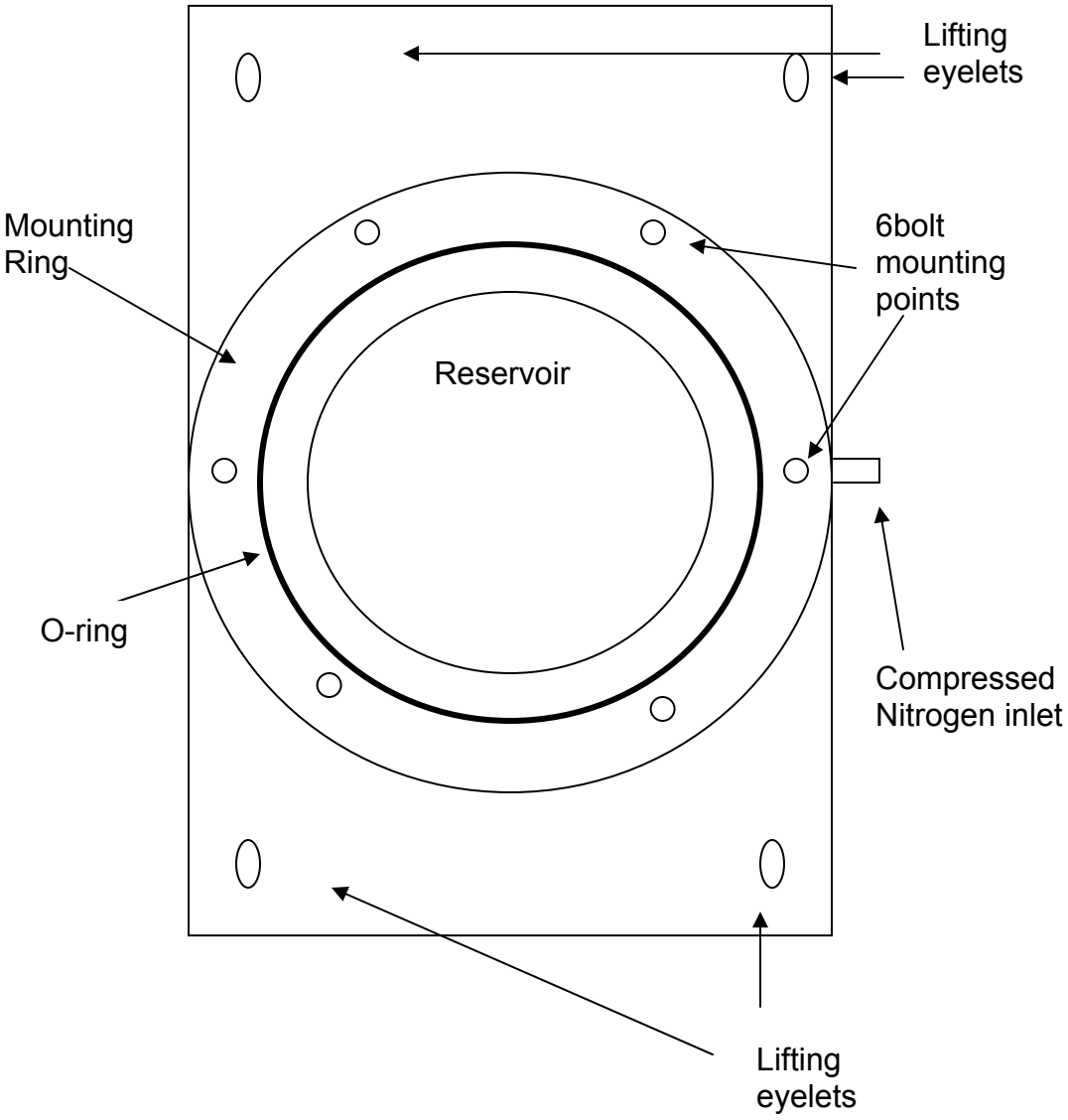

Figure III.A.2. A diagram showing a top view of the underwater toroidal bubble generator without a lid assembly. (Not to scale)

1/2-inch coarse bass screw which is permanently mounted the lid. The nozzle can quickly be changed using a standard wrench. A plug is added to the leads at the solenoid valve to again aid the quick removal of the valve in the event that a change is required.

The compressed nitrogen is added to the reservoir through a standard brass hose fitting which is threaded into the side on the bottom of the reservoir. This fitting allows for the connection of a flexible, reinforced Norprene tubing. The dimensions of the tubing are 7/16-inch outer diameter and 1/4-inch inner diameter with a safety rating of 250 psi.

Upon final assembly of the apparatus, all joints were sealed with standard aquarium sealant. This sealant was a final added protection from any intrusion of water or loss of pressure in addition to the PVC glue which was used to bond all joints. The completed apparatus is shown in figure III.A.3. A pressure test was conducted satisfactorily between 0 and17 psi. The final completed dimensions are as follows:

- Base: 42 cm x 24 cm x 2.54 cm
- Height: 22 cm (34.5 with nozzle)
- Volume 4864.4 cm^3
- Weight 7.25 Kg

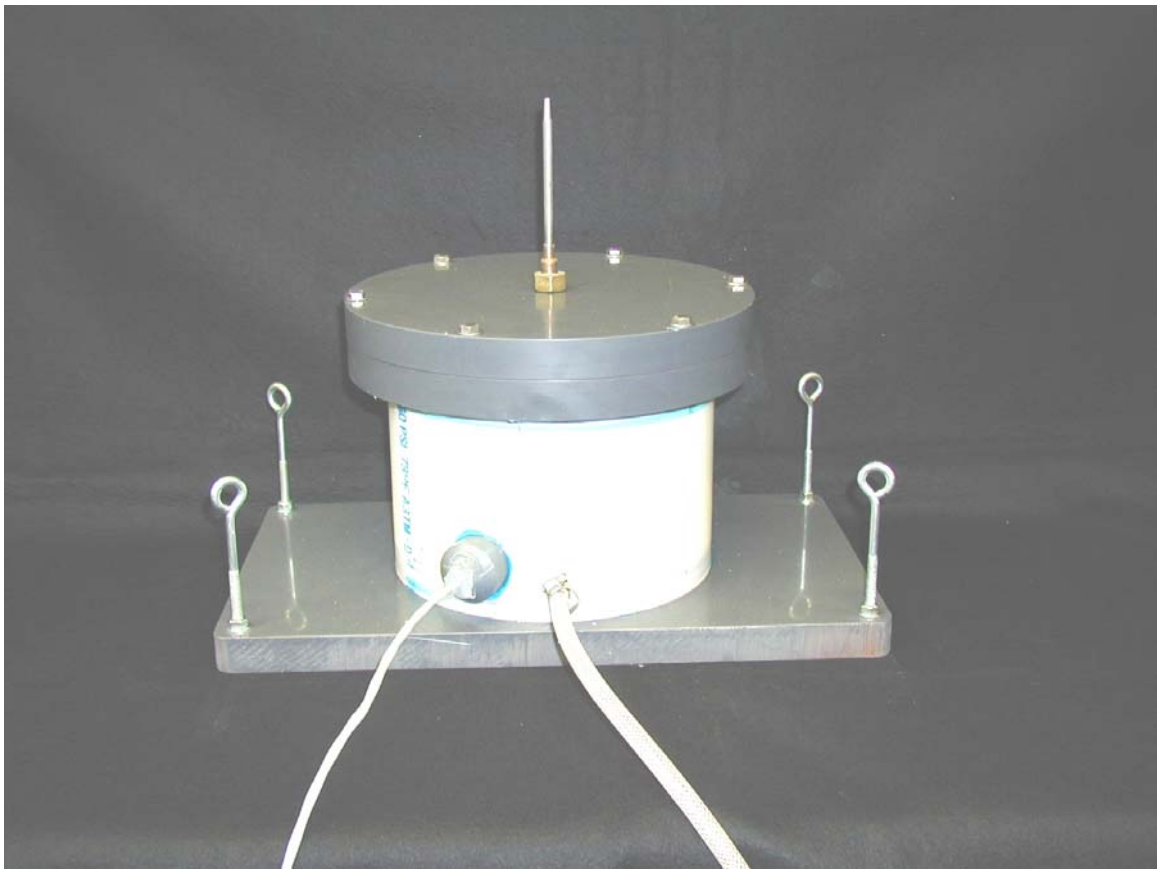

Figure III.A.3. Picture showing the completed portable toroidal bubble apparatus. Visible is the all PVC construction, the mounting of lid assembly, the compressed nitrogen inlet and the power inlet. The eyelets serve a duel use for securing weight and lifting the apparatus in and out of the water.

B. ACOUSTIC EMISSION EXPERIMENT

The acoustic emission experiment in the anechoic ocean tank utilizes all the electronic equipment that had been previously used for the acoustic noise propagation experiment (Ch.11). All of the equipment required was rack-mounted and thus easily transferred to the tank room. The underwater apparatus was lowered into the tank while pressurized to minimize any potential leakage. We positioned the nozzle tip in the center of the width of the tank but off center on the long axis so that any reflections off the walls that were experienced could be identified. The ITC-1032 omni-directional hydrophone was lowered to a depth of 1 m and centered 0.4 m away in the vertical plane which was outside of the range of possible interactions with any rising toroidal bubbles. The layout of the apparatus in the anechoic tank is shown in figures III.B.1 and III.B.2.

An ambient noise level reading was taken and is shown in figure III.B.3. The ambient noise is shown to have three frequency peaks at 15 Hz, 60 Hz and 120 Hz. The 60 and 120 Hz peaks are associated with the power distribution system and the 15 Hz could be due to the building's switching equipment or steam piping.

The next step was to determine the sound level generated by the solenoid, specifically any frequencies developed in the opening and closing of the valve plunger on the valve seat. With the portable apparatus in the anechoic tank, we triggered a solenoid burst without releasing any air. It was observed that there were two distinct voltage spikes in the time series with the second voltage peak at 63 ms after the first peak as seen in figure III.B.4. By lowering the gain level of the power amplifier to the lowest triggering setting, the second peak was observed to only be 25 ms from the initial peak so the triggering pulse did not open the valve as wide or as long. The accompanying Fast Fourier Transform (FFT) shows two frequencies at 20 Hz and 122 Hz and a broad average rise in the noise between 500 and 1000 Hz. The initial voltage peak and the second voltage peak correspond to noise emitted by the opening and closing

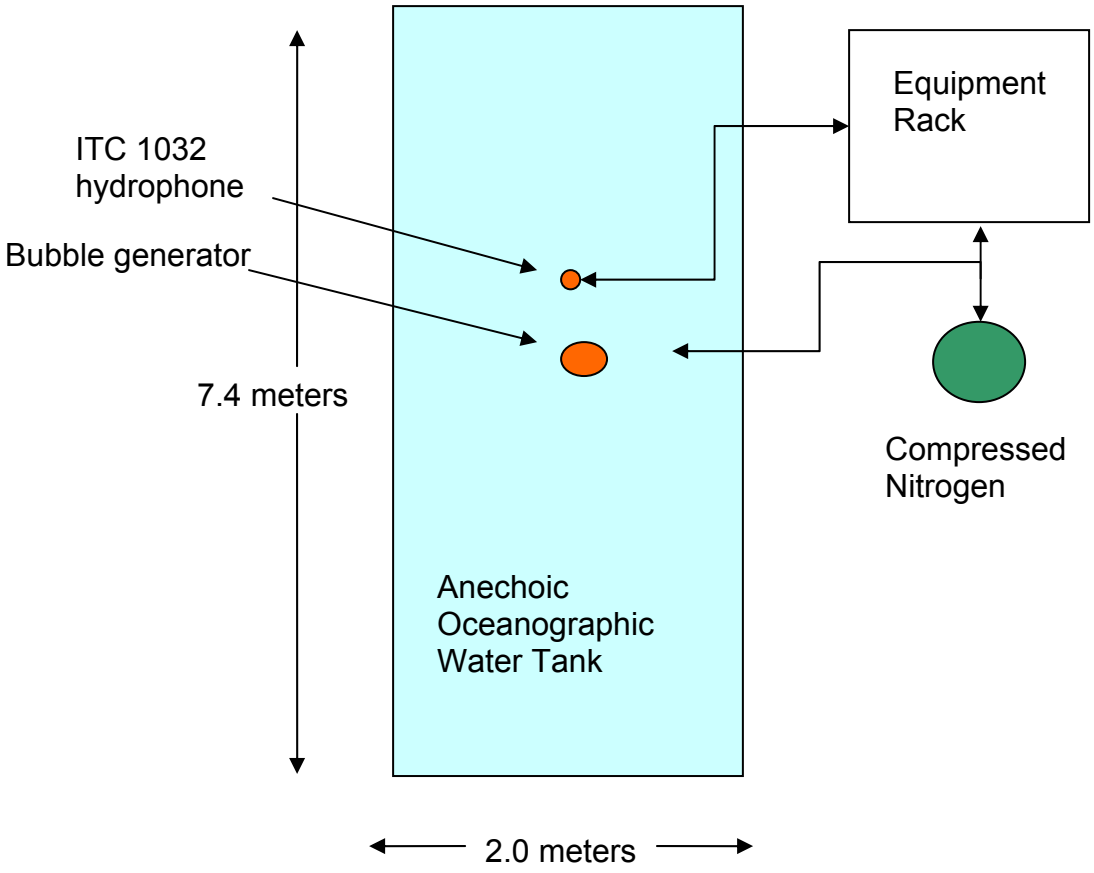

Figure III.B.1. A diagram showing the placement of the portable toroidal bubble apparatus and the omni-directional hydrophone in the anechoic water tank.

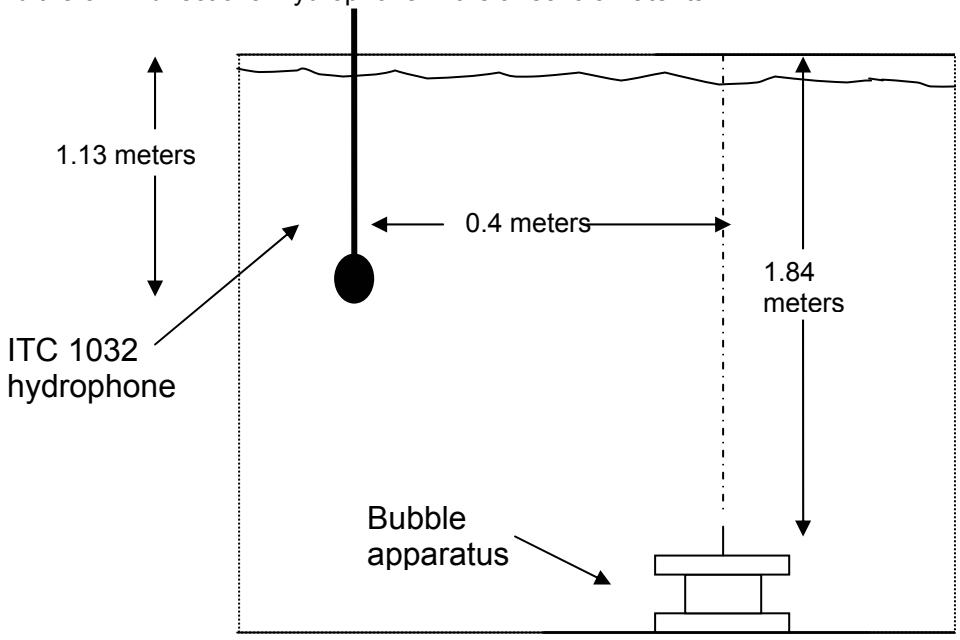

Figure III.B.2. Diagram of a side view of the portable apparatus in the anechoic tank.

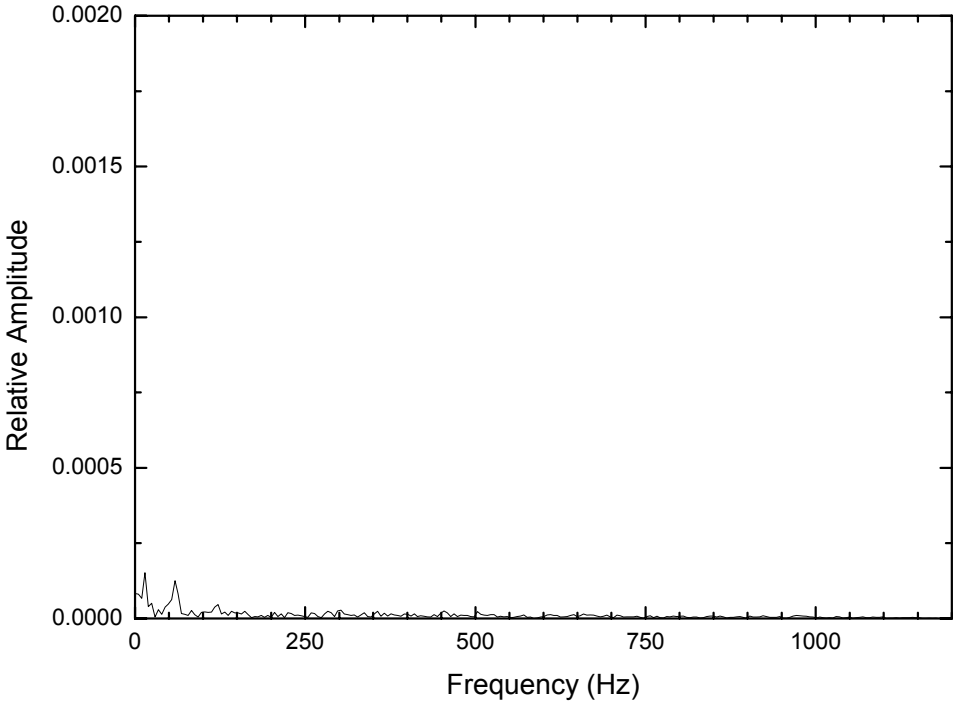

Figure III.B.3. A plot of the FFT showing the background acoustic noise as measured by the ITC-1032 hydrophone. For comparison, the vertical scale is the same as figure III.B.4.

of the valve, and there is no frequency that will interfere in the expected modes of a toroidal bubble.Reflections off the walls, bottom and top surface correspond to delay times on the order of milliseconds, and are thus part of the ring-down of the opening and closing of the solenoid valve. No negative effects of low frequency reflections were observed.

Toroidal bubbles can be classified visually, based on degree of smoothness. The most basic categorization is between smooth and rough but this can be further classified into several sub-categories. The focus of this experiment is on the initial formation of the toroidal bubble and the formation process can be categorized in much the same way. The formation of toroidal bubbles is a highly stochastic process, that is, each time the solenoid is triggered and releases gas does not necessarily lead to the formation of a toroidal bubble. Because of the short time frame of the bubble formation, roughly 100 ms based

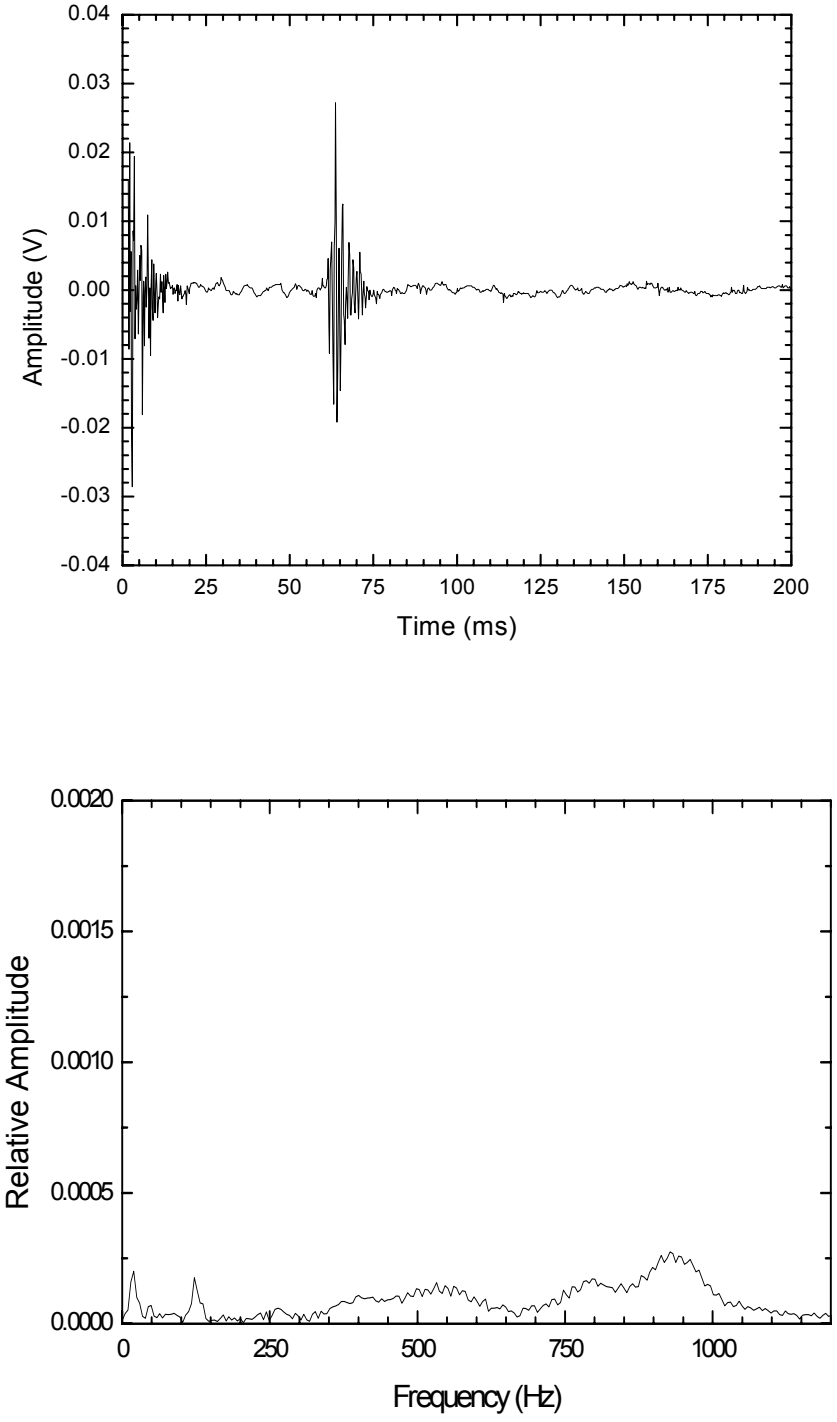

Figure III.B.4. Time series plot and FFT of a solenoid trigger without air release. Peaks at 0 and 62 ms correspond to opening and closing of the solenoid valve, respectively.

off observation, we only look at the initial state of the air burst from the tip of the nozzle. If a toroidal bubble is observed, the data is classified into the basic category of smooth or rough. In the event that no toroidal bubble is observed, the air burst from the nozzle can be classified into toroidal formation with immediate break-up and spherical cap bubbles only when no toroidal formation is apparent.

In the case of a toroidal formation with immediate break-up, the air burst leaves the nozzle tip in a toroidal vortex ring. This vortex ring is generally the same size and shape as the vortex rings which form toroidal bubbles. The observable difference is that in the case of immediate break-up, the vortex ring appears to be made up of smaller spherical bubbles. In the time frame of tenths of a second and a travel distance of centimeters from the tip of the nozzle the vortex ring collapses into multiple spherical cap bubbles and spherical bubbles of various sizes. In the second classification of spherical caps only, it is observed that there is no apparent vortex ring type formation from the tip of the nozzle. The observed air burst is turbulent and breaks immediately into spherical bubbles and spherical cap bubbles.

For the experiment, the pressure of the incoming nitrogen was set to 3.5 psi and the HP 33120A function generator was set to 70 Hz in the burst mode. In the cases were a smooth toroidal bubble forms, it can generally be seen from the time series plot that a sinusoidal signal starts at approximately 50 ms from the lifting of the valve and just before the second peak associated with the closing of the valve. When an FFT of the data is taken, generally there is a large single frequency peak between 150 and 250 Hz as seen in figure III.B.5. This is not always the case as multiple peaks which are closely spaced in frequency can occur. Also, there are smooth toroidal bubbles with much longer rise times on the order of double the rise time of other smooth and rough toroidal bubbles. They occur very infrequently, roughly one out of every thirty toroidal bubbles generated and generally, they become very thin as they rise in the water column. The time series plot of one of these extremely smooth types does not have a ring

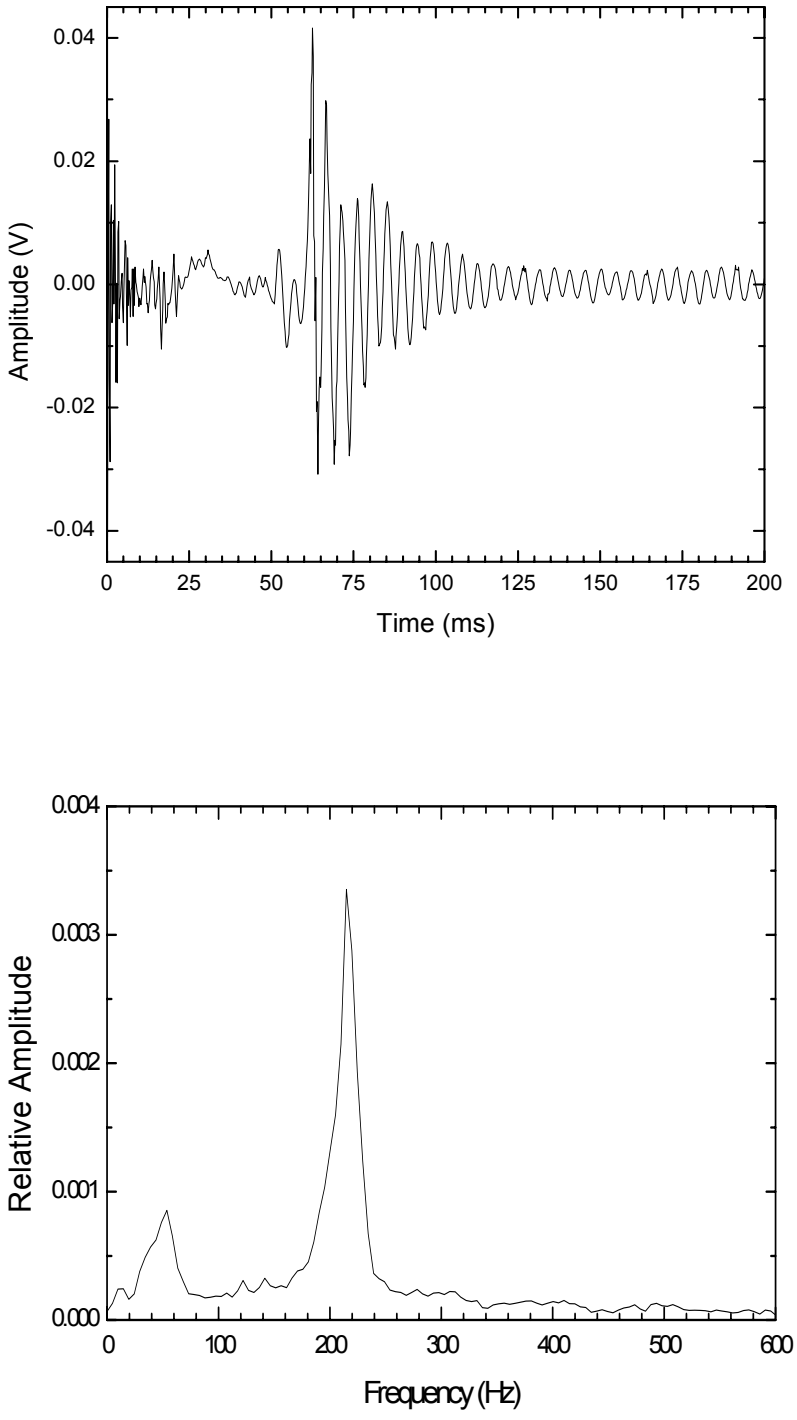

Figure III.B.5. Time series plot and FFT of a smooth toroidal bubble. There is a single frequency peak at 215 Hz

down feature like the standard smooth bubble plots and the FFT shows a broad frequency rise from 150 Hz to 250 Hz as seen in figure III.B.6.

In the case in which there is smooth toroidal bubble with a double frequency peak observed in the FFT, beats are seen in the time series plot. In the example of figure III.B.7 the primary peak is at a frequency of 244 Hz and there is secondary peak is at 215 Hz. The beat period is approximately 35 ms and can be calculated from the difference in the frequency peaks.

There is very little ring down observed in the smoothest toroidal bubbles and a typical example of an extremely smooth long duration bubble is shown in figure III.B.7. The FFT plot shows the same rise in amplitude between 150 and 250 Hz as seen in a smooth example but unlike the observation with the typical smooth example the is no strong single peak. In the time series plot the same large that the spike is observed at the closing of the solenoid valve but there is no ring down effect and the amplitude of the sinusoidal signal is much lower.

Figure III.B.8 is a typical example of a rough toroidal bubble time series and FFT plot. The time series plot in this example is similar to the smooth bubbles with a ring down effect but the amplitude can vary from bubble to bubble with some displaying the characteristics of the smoothest examples. The FFT plot typically has two major peaks in the frequency range between 150 and 250 Hz and two minor peaks at 210 Hz and an outlying peak above 300 Hz. In this example the main peaks are 180 Hz and 235 Hz with another minor frequency peaks at 210 and 503 Hz.

Shown in figure III.B.9 is an example of an immediate break-up type air burst. The time series plot typically show the signal starting 40 to 50 ms and ringing down after the valve closes at 63 ms. The sinusoid signal is similar to the smooth or rough examples. The FFT plot shows a typical structure which is characteristically similar to the rough toroidal bubble examples. Two major frequency peaks are seen between 150 and 250 Hz and there are peaks at 210 and an outlying peak above 300 Hz. In the example shown in figure III.B.9 the two primary peaks are 171 and 220 Hz and the minor peaks are at 210 and 420 Hz.

The final example shown in figure III.B.10 is a burst which did not produce an apparent toroidal formation and only cap bubbles were observed leaving the nozzle. The time series plot signal displays smaller amplitudes after the closing of the valve. This is very similar to the extremely smooth example of figure III.B.7. The FFT plot typically shows a single frequency peak between 150 and 250 Hz like the smooth examples (Fig B.7).

From the data collected on the smooth toroidal bubbles, the single frequency peak from the FFT decreases in amplitude for bubbles of increasing smoothness and the sinusoidal signal has a smaller amplitude. The examples which can be classified as extremely smooth have very little ring down and have a reduced single frequency peak. This is the opposite of what we expected which was that the smoothest bubbles modes would be the most excited. It is the case that the smoothest bubbles have no modes excited. The air burst which produces a smooth bubble must have a smooth flow. The examples where beating is observed could possibly be explained by volume modes of the inner and outer surface of the air cloud before punch trough and creation of the vortex ring. This would have to be confirmed by high speed photography.

In the case of the rough toroidal bubbles, there are typically two main frequency peaks in the FFT between 150 to 200 Hz and 210 to 240 Hz. There is also an outlying smaller frequency peak above 300 Hz. The double peak indicative of a broken and turbulent nature to the air blast and of the higher frequency may be a volume mode of the rough toroidal bubble as they typically have a larger diameter than the smooth. As seen in the data, the immediate break-up type bubble has a similar FFT plot structure and this agrees with the visual observation that the vortex ring that creates both types are similar.

Solenoid triggers that do not produce an apparent vortex ring have similar time series plot and FFT structure as the smooth bubbles. Based on these observations, we must conclude that a vortex ring is created but not apparent to an observer. This should be confirmed by correlation to high speed photographs in the future. There is no precursor signal apparent in either the time series voltage plot or the FFT which could determine the future fate of the air burst on

triggering of the solenoid. It is clear that there is a frequency difference between smooth and rough toroidal bubbles due to differences between a laminar flow and turbulent flow formation. This could lead to future work in the acoustic emission of turbulent flow in thunderstorms and the classification of vortex rotation as smooth or rough based on frequency.

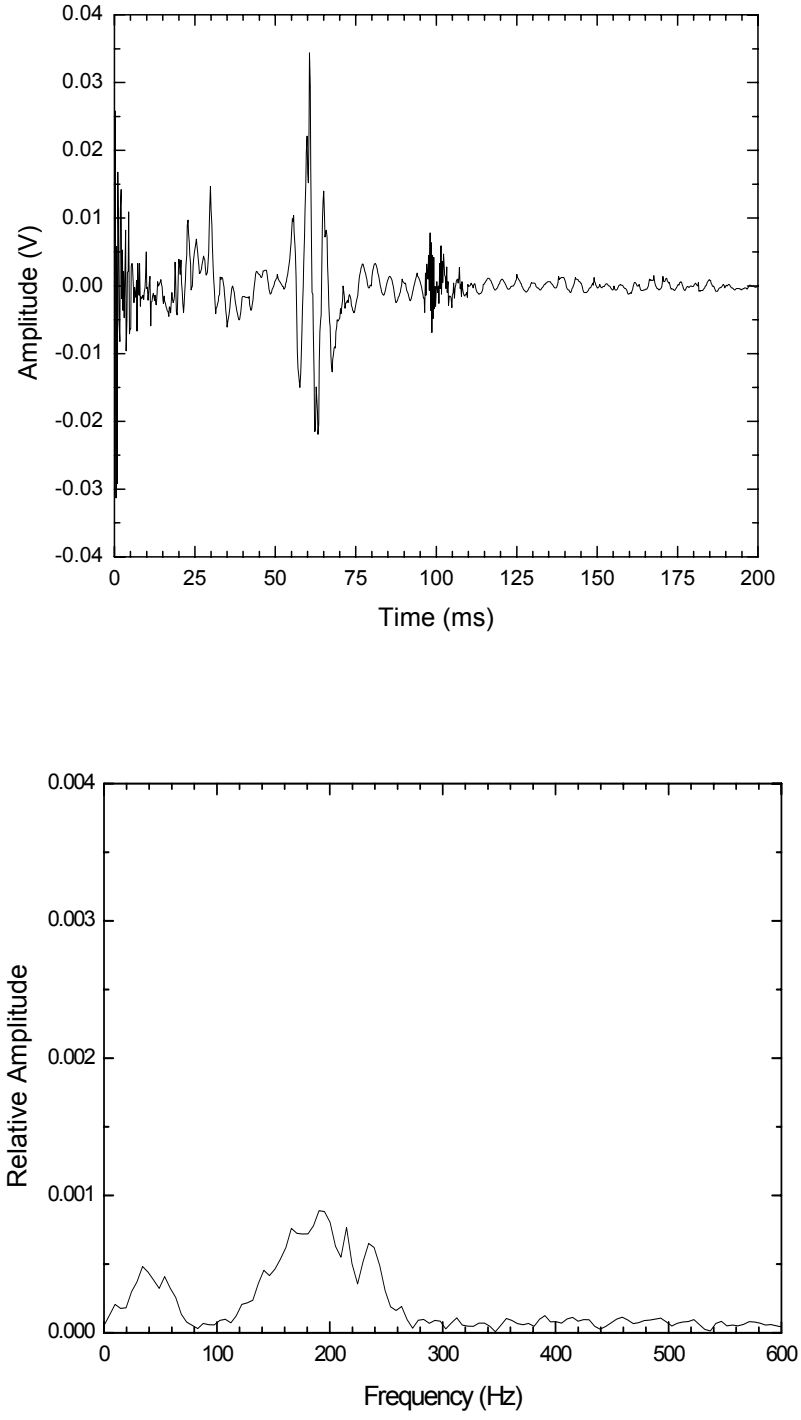

Figure III.B.6. A toroidal bubble that is extremely smooth. There is a lack of a ring down in the time series plot and in the FFT it can be seen that there is a separate distinct peak at 215 Hz with a relative amplitude much lower than with other smooth bubbles.

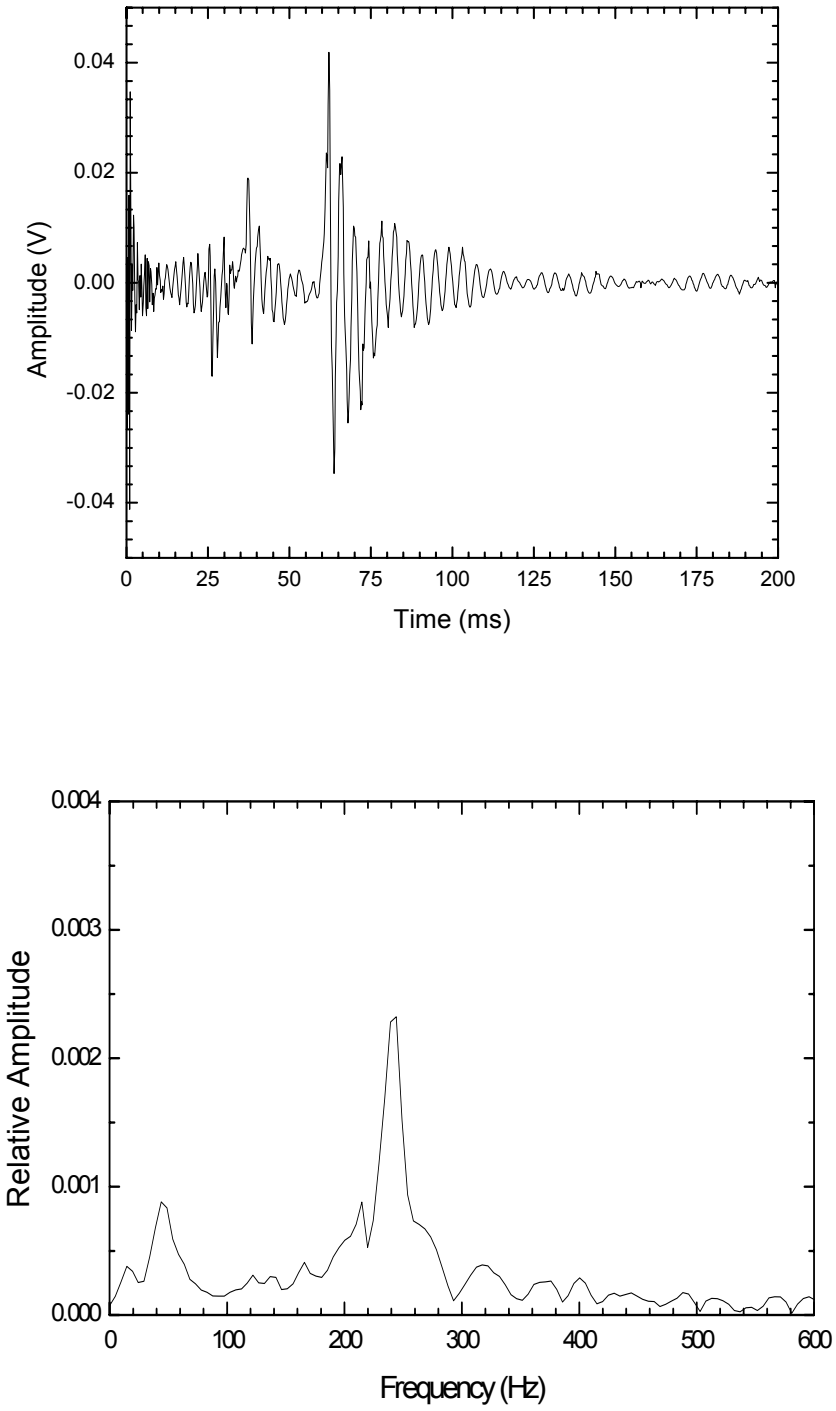

Figure III.B.7. An example of a smooth toroidal bubble two frequency peaks in the band between 150 and 250 Hz. The 215 is a secondary peak to the 244 peak. Beats between these two frequencies are observed in the time series plot starting at 120 ms.

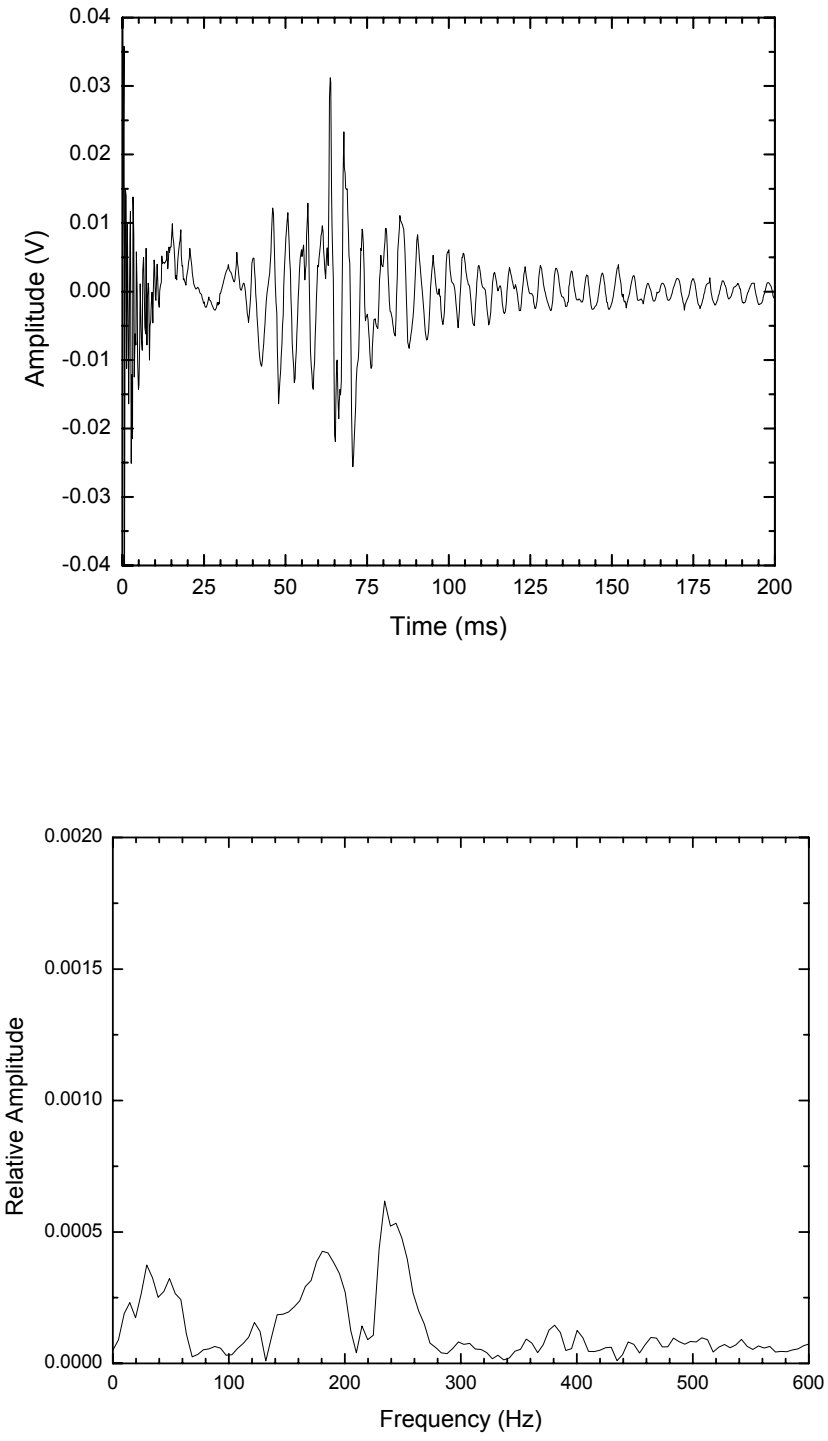

Figure III.B.8. An example of a rough toroidal bubble with two frequency peaks in the band between 150 and 250 Hz. At 180 and 235 Hz.

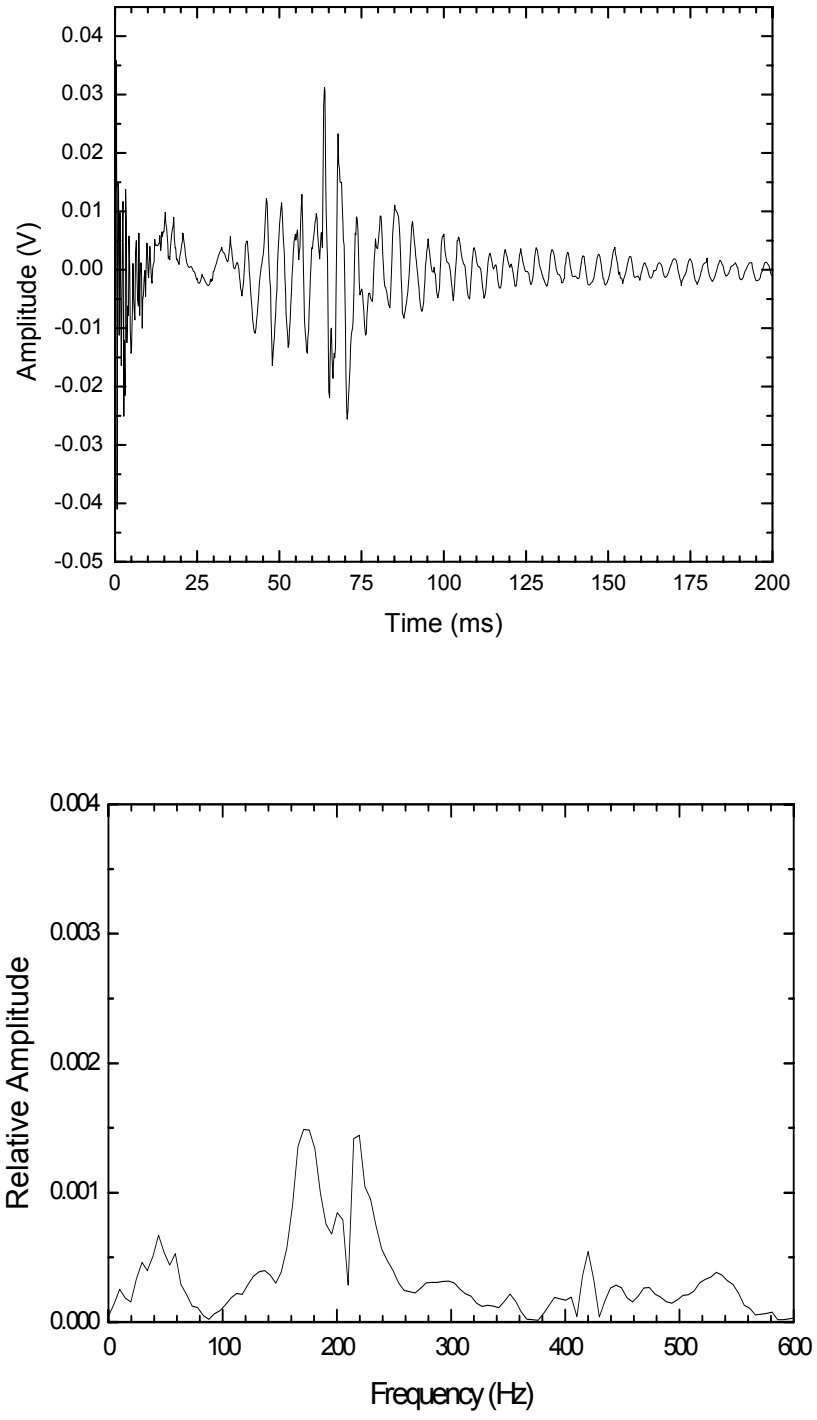

Figure III.B.9. Time series and FFT plot of a toroidal bubble of the immediate break-up type. The structure of the FFT is similar to the rough bubbles with peaks at 180 and 235 Hz.

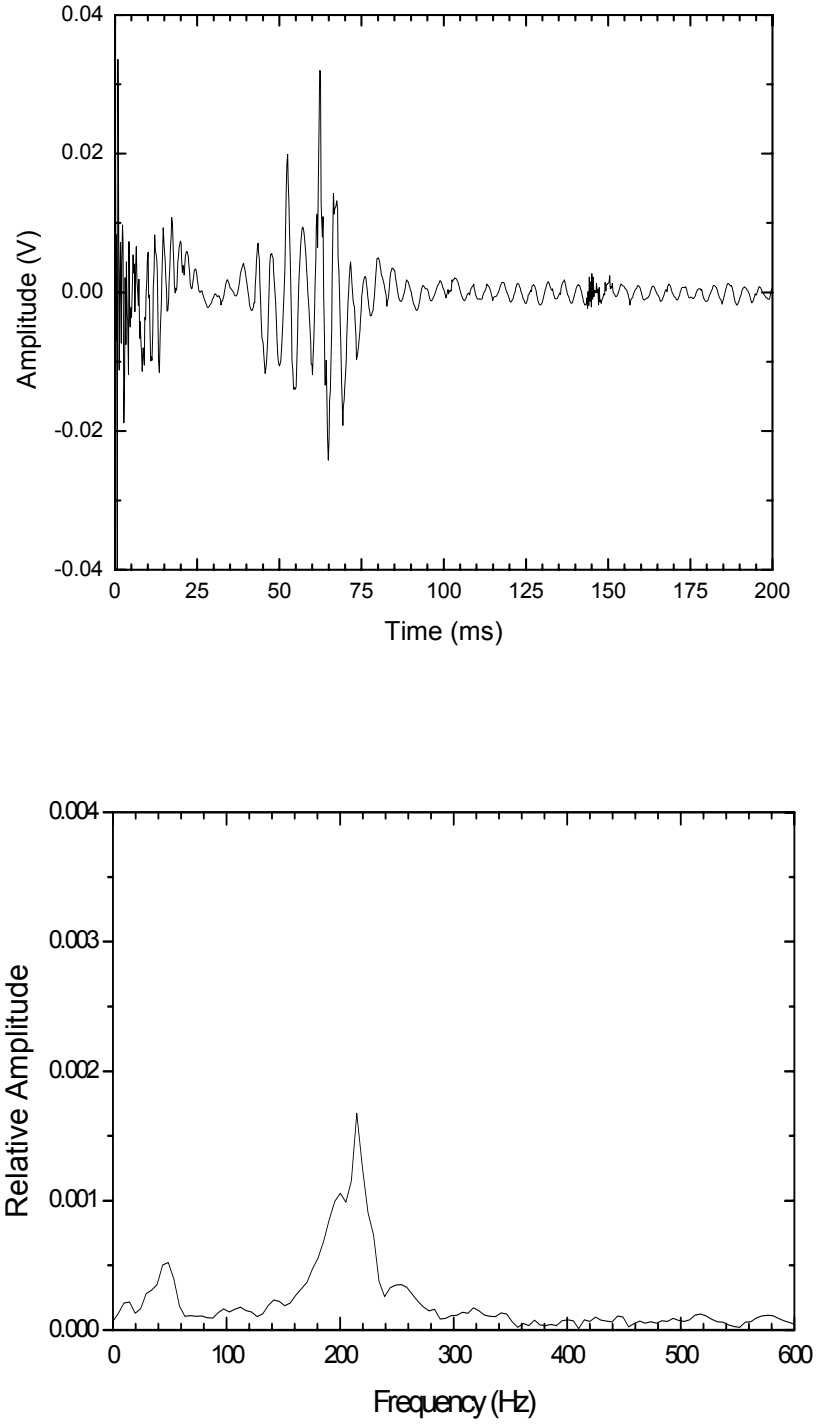

Figure III.B.10. Time series and FFT of a solenoid fire in which no toroidal bubble was observed. It has a similar structure to the smooth bubbles with a peak at 215Hz.

C. ACOUSTIC SCATTERING EXPERIMENT

The underwater apparatus was set-up in the anechoic tank to investigate the scattering properties of a smooth toroidal bubble in its horizontal plane. The portable bubble generator was placed in the same location in the anechoic tank as in the acoustic emission experiment (Fig. III.B.1). The ITC-1032 hydrophone was suspended at a horizontal distance of 1.0 m from the generator and at a depth of 1.0 m (midway between the top and the bottom of the tank). The flexural disk transducer (FDT) from the propagation experiment (Ch. II) was placed 2.0 m on the opposite side of the bubble generator and at a depth of 1.0 m. Noise from the HP33130A function generator was band-passed between 250 Hz and 1200 Hz with the SR640 filter. The applied voltage to the FDT was 270 V_{rms}. A pressure of 3.5 psi was supplied to the portable generator.

The received time series signal was triggered by hand when a smooth toroidal bubble was approximately in the horizontal plane of the FDT and hydrophone (depth of 1.0 m). This is well after the acoustic emission has occurred (Sec. III.B), which was verified with the noise off. Due to the high viewing angle, the triggering occurs when the bubble is in the horizontal plane with an uncertainty of ±10 cm. We recorded and averaged 64 trials of time series of the noise in the absence of a toroidal bubble, and 64 trials of the noise in the presence of a smooth toroidal bubble. The spectrum of the averaged time series in the absence of a toroidal bubble is shown in the top graph of Fig. III.C.1, and the spectrum of the averaged time series in the presence of a toroidal bubble is shown in the bottom graph.

The data in both graphs roll off as the frequency decreases to 750 Hz, which is due to the resonance of the driver. Below 750 Hz, in the region of the resonance frequency of the toroidal bubble, the signal does not rise above the ambient noise floor, which masks any effect of scattering. The experiment thus suffers from the fact that the driver cannot achieve a sufficient amplitude at the requisite low frequency. However, the data show an interesting feature.

From 1000 to 1200 Hz there are roughly twice as many peaks of the spectrum with a toroidal bubble compared to the spectrum without a toroidal bubble. The geometrically calculated frequency above which the walls are absorptive is roughly 10 kHz, so the peaks in the spectrum without a toroidal bubble could be due to standing wave modes of the tank. Calculations of the standing wave frequencies support this. We do not understand how a toroidal bubble could cause any increase in the number of peaks. One possible explanation of the results is that an insufficient number of averages was taken, although 64 would appear to be sufficiently large to smooth out any peaks due to fluctuations. The next step would be to increase the number of averages and ascertain whether the increased number of peaks persists.

An alternative experiment of the absorption of sound by a toroidal bubble is to drive a standing wave mode of the tank at a pure frequency rather than noise. Although it is extremely improbable that any standing wave frequency will equal the resonance frequency of a toroidal bubble, there is expected to be a small but perhaps measurable shift in the resonance frequency of a standing wave mode.

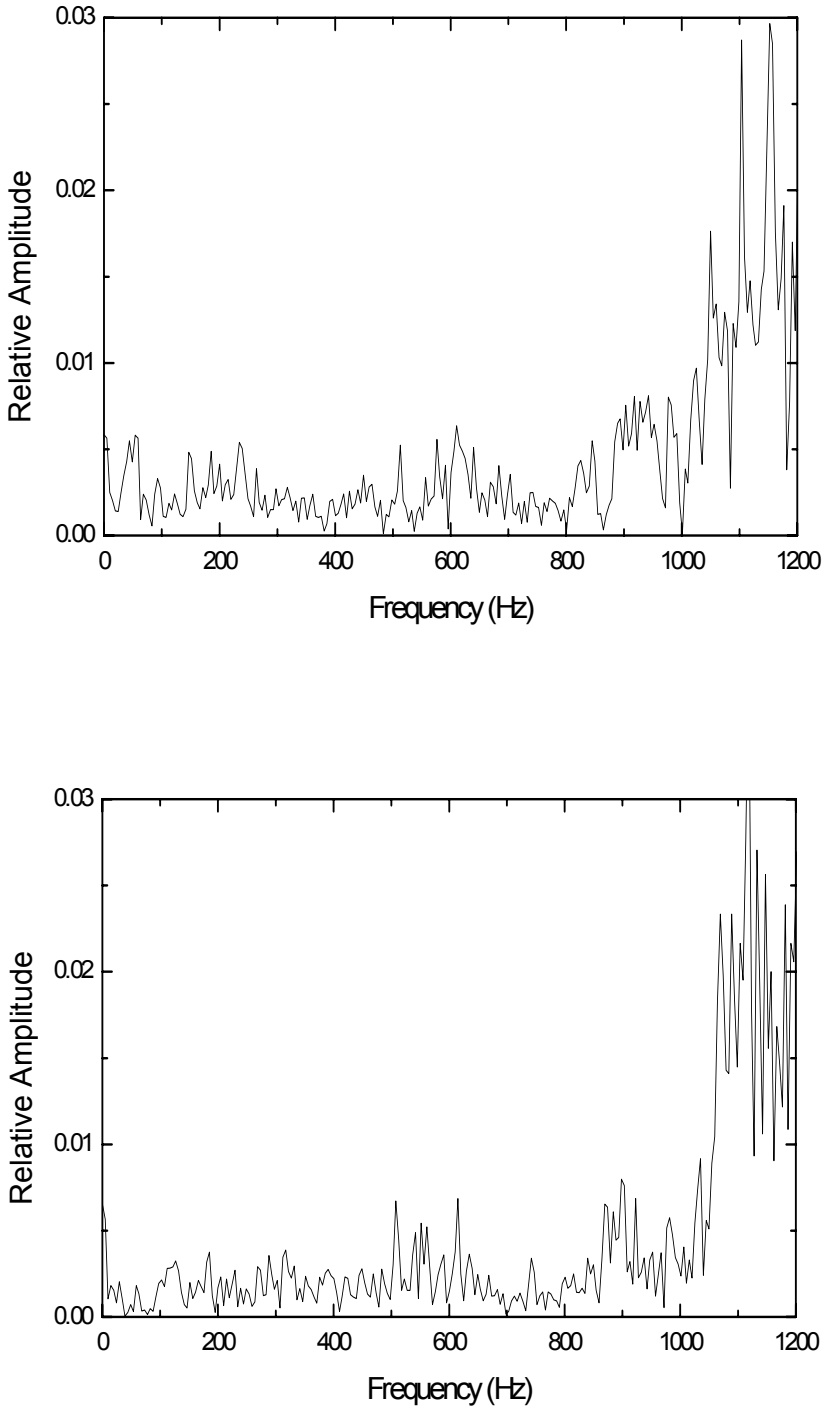

Figure III.C.1. Top: Spectrum of a time average of the received noise signal with no toroidal bubble present. Bottom: Spectrum of a time average of the received noise signal with a smooth toroidal bubble present.

THIS PAGE INTENTIONALLY LEFT BLANK

IV. LARGE APPARATUS

In the prior two chapters there were several deficiencies in the available apparatus used. The acoustic propagation experiment in chapter II was limited by the small size of the water tank in both diameter and height preventing the use of larger acoustic transducers. Also, the circular nature of the tank creates significant problems of reflection and distortion when trying to take photographs of bubble development. For the acoustic emission and scattering experiment of chapter III, there were no side viewing portals so the operator was forced to view the bubbles from a high angle. The height of the toroidal bubble as it rises in the tank could only be estimated for the scattering experiment and it was impossible to take necessary high speed photographs needed to correlate the evolution of the toroidal bubble formation to the observed acoustic emission. We determined that a new apparatus was required for future work which would correct these deficiencies. We also wanted to construct a hallway apparatus for hands-on use by the public, and we realized that the same apparatus could serve both purposes.

A. CONCEPT OF DESIGN

In designing a new apparatus we wanted it to operate in the same manner which had been developed by Hobbs (2000). This operation, as previously described, uses an electrically operated solenoid valve to release a burst of compressed nitrogen from a charged reservoir through a specially shaped nozzle which creates a toroidal bubble in the water. A second requirement for the tank was flat side construction for distortion and reflection free high speed photography. We also wanted the tank to be significantly larger in both height, for increased bubble rise time, and in width so larger transducers could be used for further work in acoustic emission and scattering. Lastly, the tank must be large enough that there would be no boundary effects due to the tank edges. The size of the tank would make it visually interesting so that the apparatus could

have a dual use as a public display. Compressed air can be provided by the building medium pressure air supply. Figures IV.A.1 and IV.A.2 show the concept of the apparatus.

The practical limit to overall height of the apparatus is 9 feet. This height would allow for ceiling clearance while at the same time providing a space for the addition of any required sensors. Based on this, we decided on a tank height of 6 ft and 2.5 ft for the stand height which would leave 1.5 ft clearance above the tank. The diameter of Hobbs' apparatus is 1 ft which leaves little room for sensors to be located at any position other than the top or bottom when in operation. We decided that the new tank would be 2 ft by 2 ft which would allow for the placement of hydrophones at any required depth during operation without interference to the bubble. This size would also be large enough, based on our experience, to prevent any negative boundary effects due to the square shape. Because of the 6 ft height of the tank would make glass impractical due to weight, clear acrylic was chosen for the tank wall material. Acrylic has several advantages over glass for water tank construction: its lighter weight will ease any moves required, the acrylic cannot be broken by public abuse, and the construction of the tank is much simpler and stronger. Due to the weight of the water in a tank of this size the stand would have to be of sturdy steel construction capable of carrying a load of 2000 lbs.

We considered two options for designing the solenoid/reservoir assembly for the large apparatus. The first option was to construct the assembly in the manner as was done for Hobbs with the solenoid and reservoir located in the stand beneath the apparatus. This has the advantage of allowing of quick changes of the solenoid valve and removal of the reservoir for inspection. A second option is to build the assembly as in the manner that was done for the portable apparatus in chapter II with the reservoir housing the solenoid and nozzle in the water tank. There are several disadvantages to this method: the solenoid could only be changed by draining the tank, a drain would have to be added to remove any water which intrudes into the reservoir, a sight glass would need to be added to observe the water level, and the travel time of the toroidal

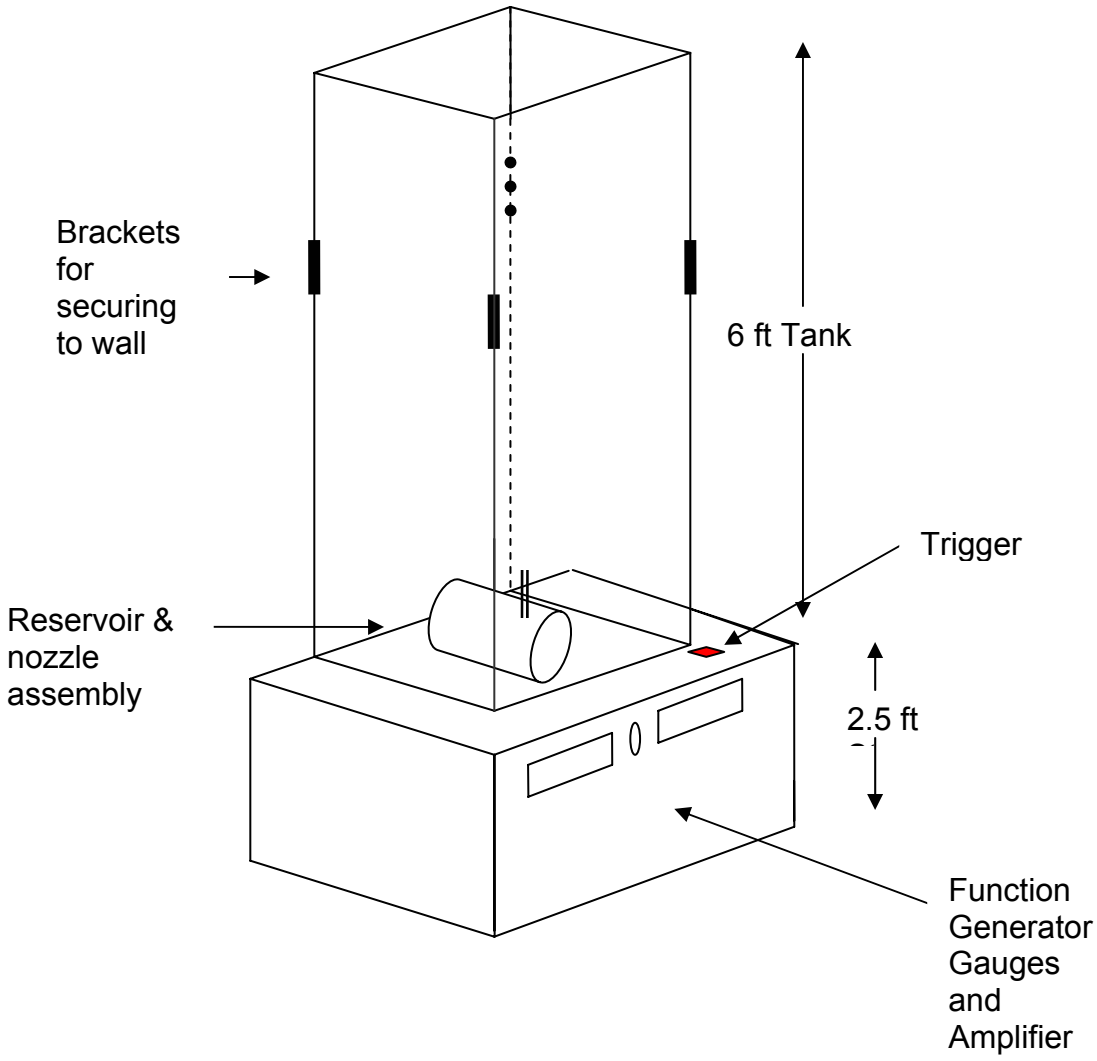

Figure IV.A.1. Concept diagram for large apparatus.

bubbles is reduced. The advantage of this method would be the visual impact on the general public in being able to view the source of the toroidal bubble thus we decided on this method.

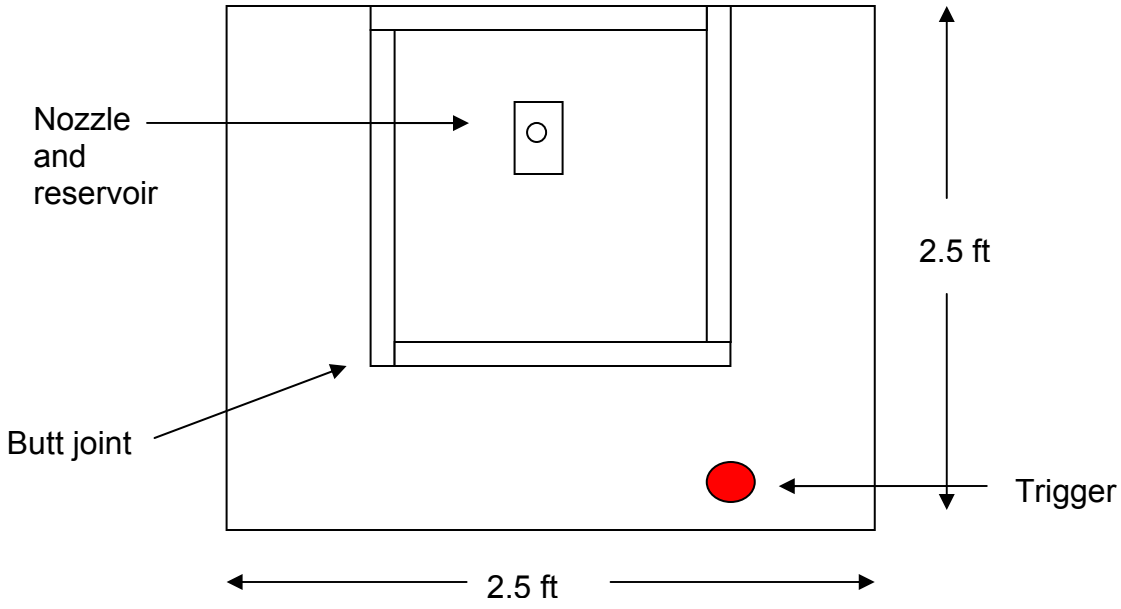

Figure IV.A.2. Top view of tank showing location of tank in relation to the stand and the butt joint wall construction.

B. CONSTRUCTION

Copper tubing with a diameter of 6 inches was cut to a length of 6 1/4-inches to act as the reservoir housing. Two pieces of brass angle 6.5 inches long were added to the base to act as a stand and we secured to the base of the tank with mounting bolts. In the top of the reservoir, two brass fitting were added. The first is a double male thread fitting that is 5/8-inch on top for adding the nozzle and a 5/8-inch in the reservoir for screwing on the solenoid. The second fitting is a female 1/2-inch thread fitting for the compressed air. Both fittings were brazed to create a leak tight seal. Standard copper tubing typically used for household hot water operations were added to the bottom to act as a water drain and to the side to act as a wire run for the solenoid power leads.

The end caps for the cylindrical reservoir are made of 0.5-inch clear acrylic cut circularly to 8-inches diameter. A grove is cut into the inner face of the

acrylic 6 inches in diameter for the addition of an O-ring at the copper acrylic interface. An O-ring of this type proved highly effective for the portable apparatus. The seal is created by six equally spaced bolts connected with a 7.5-inch long 1/4-inch threaded rods. The completed generator assembly is seen in figure IV.B.1 and figure IV.B.2.

Four sheets of 2 ft by 6 ft clear 1/2-inch acrylic sheets are glued together in butt joint fashion to create the tank walls. Acrylic cement, methylene chloride, is the bonding agent. The acrylic wall was machined at the factor to a tolerance of ± .005 inch. This fine machining enabled us to use a capillary action cementing technique. This cement technique evenly fills the joints to create the strongest possible acrylic bond. For added strength, 13 screws per corner were added along each of the butt joints. These screws are 10/32 by 1 inch fine thread screws and are spaced 6 inches along the joints starting 1 inch from each corner. The tank bottom is constructed out of 1 inch thick PVC 2.5 by 2.5 ft in size. A 0.5 inch deep 1/2-inch groove is cut into the plate to receive the tank. The grove was then sealed with epoxy and all joints top coated with a bead of silicone as final protection against leaks. Three fittings penetrate the bottom: an air line, copper water drain line and the power leads for the solenoid. All are sealed with PVC glue and a silicone bead.

The stand is constructed out of heavy gauge steel angle iron in a box construction with the bottom horizontal supports 0.5 ft from the floor. For added structural integrity, two diagonal cross pieces of steel are welded to each vertical space. The stand's overall dimensions are 2.5 by 2.5 by 2.5 feet, with the over-size providing added stability to the tank. A single 1/4-inch steel plate acts as the table top. A wooden shelf is included for the required electronic equipment to include the HP33120A function generator and a triggering amplifier. A thin clear acrylic cover is added to all sides to prevent unauthorized access to the electronic equipment and the front cover piece is hinged to allow for operator access.

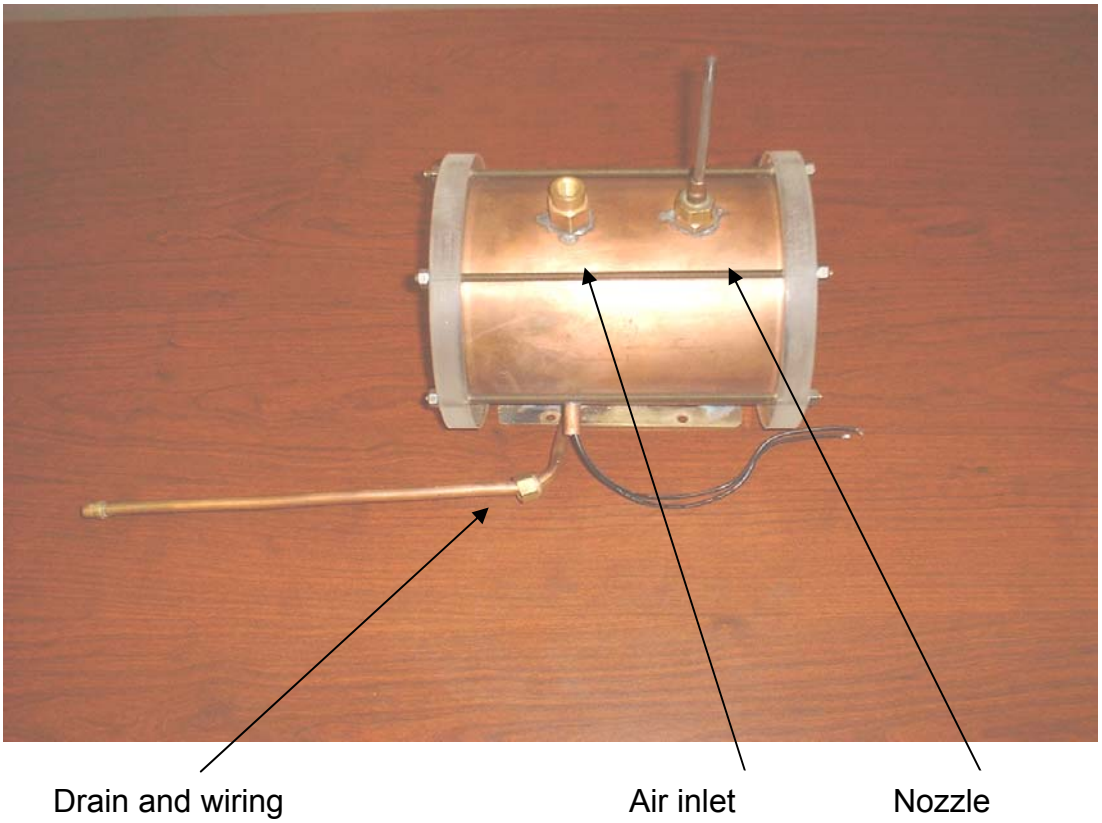

Figure IV.B.1. Bubble generator assembly. All fittings can be seen. The bottom is the water drain and wiring outlet. The top two fittings are the compressed air inlet and the nozzle.

An external triggering button was added to the table top which can connect to the external triggering port of the HP33120A function generator. The trigger is a finger touch pressure bar connected to a simple circuit containing a 4013 flip flop and a capacitor. By pressing the bar a solenoid triggering pulse is sent based on the current settings on the function generator. The circuit allows for quick multiple firings and it prevents a continuous pulse signal if the bar is held down.

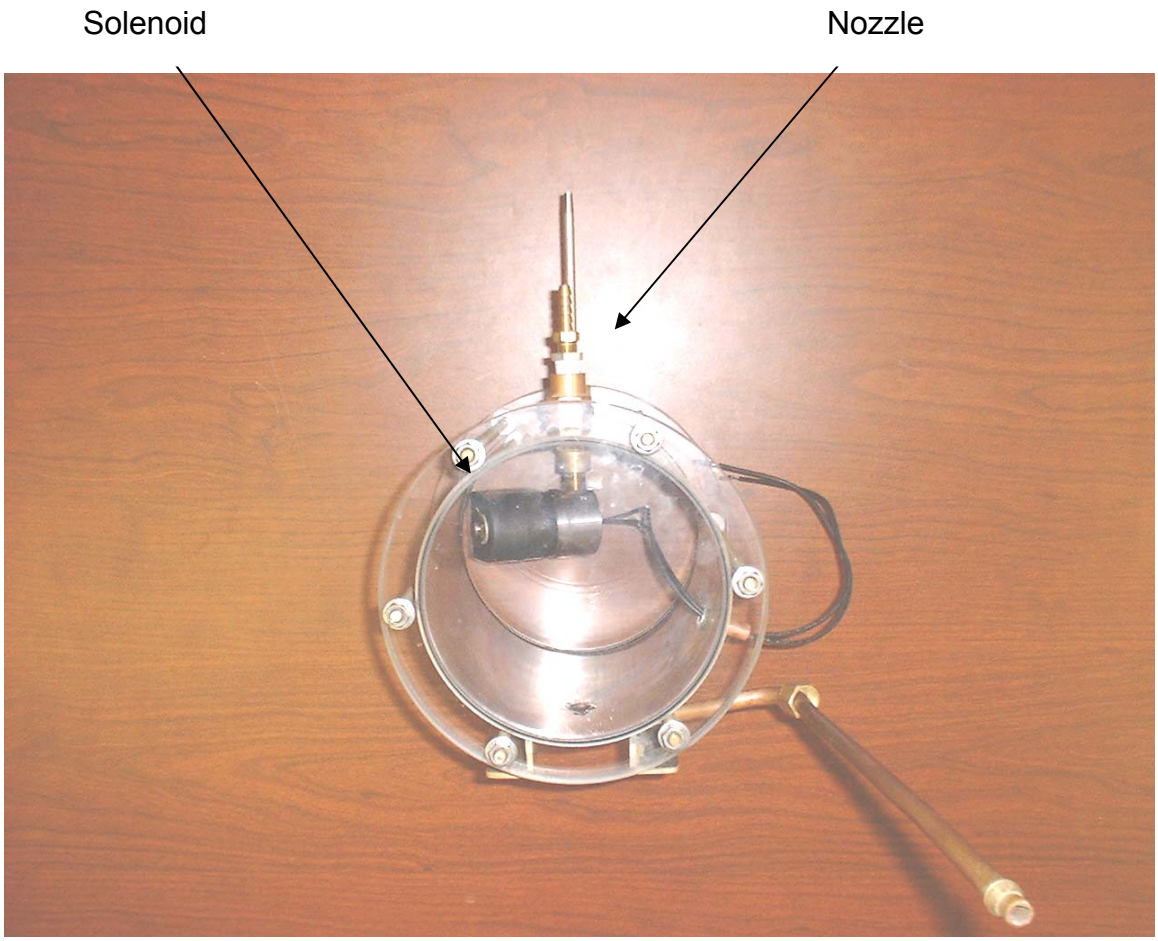

Figure IV.B.2. Bubble generator assembly in a side view (main public viewing angle). The solenoid is clearly visible as are the 6 securing bolts. Copper drain is at bottom.

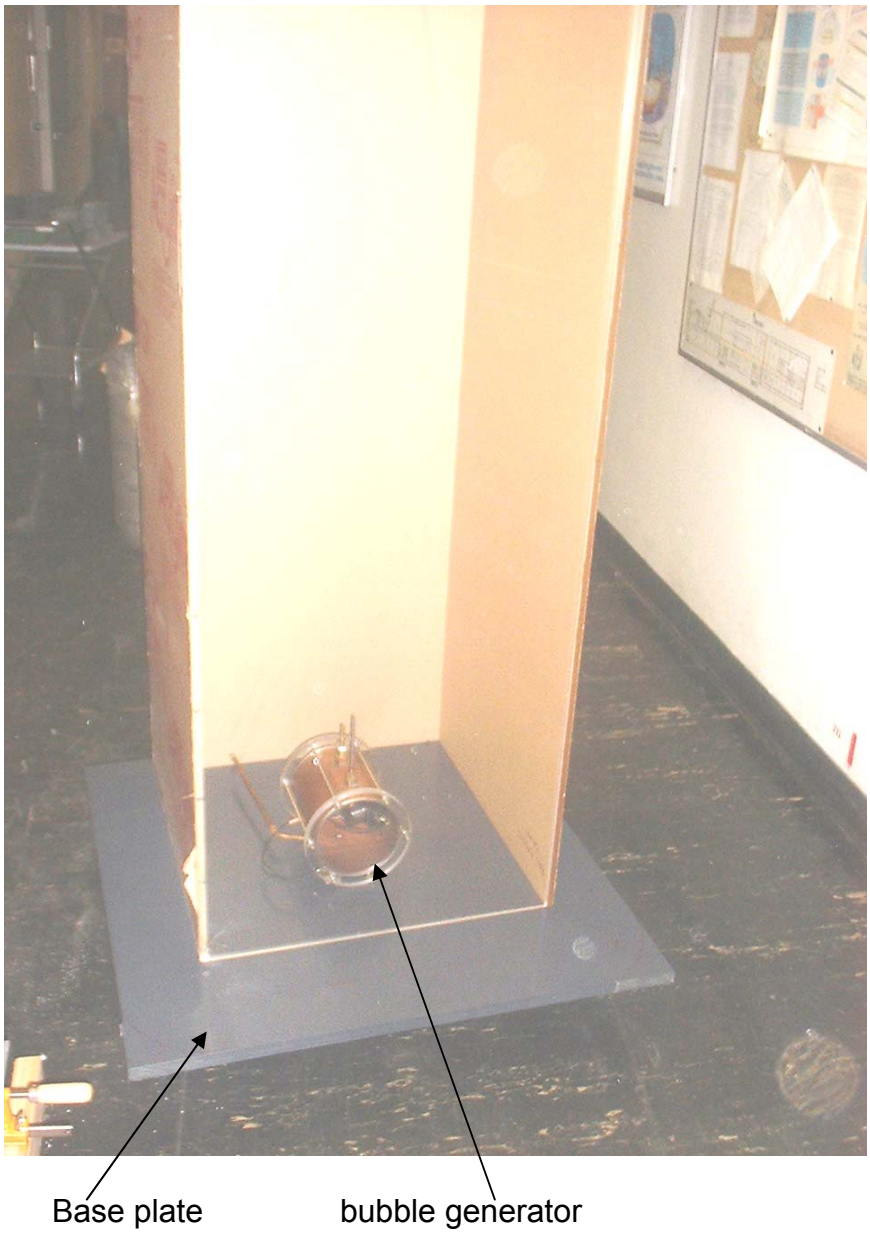

Figure IV.B.3. Large apparatus tank with bubble assembly. Three sides of the tank covered in protective paper. Steel stand not shown.

V. CONCLUSIONS AND FUTURE WORK

A. CONCLUSIONS

The acoustic drag experiment did not produce the desired result of increased acoustic drag becoming measurable as an increase in the average rise time. For a count of 60 bubbles under ambient and noise conditions there was no difference in the mean rise times. It was expected that the noise band would increase the rise time by increasing the drag on the bubble. Based on the estimate of 650 Hz for the bubble resonance, the noise was passed between 250 Hz and 1200 Hz because the Einstein-Hopf Drag effect requires an overlap of the bubble's resonance width (Larraza and Tucholski, 2000). The lack of positive results could be due to several limiting factors of the apparatus and available equipment. The size of the apparatus limited the size and configuration of transducer which could be place in the tank. The intensity may not have been sufficiently high. Also, the band selection used may not have covered the required resonance overlap and due to the roll-off nature of piezoelectric transducers the noise bandwidth may not have been homogeneous at the lowest frequencies. In a preliminary experiment, a negative physical effect was observed in which the transducer could vibrate the solenoid valve open at high power negatively skewing the results. Any future experiment must contend with this possibility.

There are several surprising results seen from the acoustic emission experiment. Contrary to a prior assumption, as smoothness of toroidal bubbles increase, the acoustic emission decreases. The formation process for these types of bubbles apparently is approximately laminar and the volume mode is excited very little. Smooth toroidal bubble examples are also seen which show a beating frequency in the ring down. This is possibly cause by the two different volume mode oscillations in the toroidal bubble. Bubbles which are classified as

rough have a very similar frequency structure to those which break-up prior to the formation of a coherent toroidal bubble. Air bursts which lead to these types of formations have a turbulent nature and the stochastic process of formation produces a coherent rough toroidal bubble or one that breaks-up into cap and spherical bubbles.

We did not observe an acoustic emission which could be identified as a precursor to the future development of the air blast. The formation process is very fast, tenths of a second, and any predictive element provides at most this much advanced knowledge. However, a predictive signal is still important because it would serve as an analog to prediction of tornadoes, which evolve on a much longer time scale. The initial signal can be classified, to a reasonable degree of accuracy, between smooth and rough toroidal bubbles by only observing the frequencies from the FFT.

The scattering properties of a smooth toroidal bubble in its horizontal plane were investigated in an anechoic tank and no effect was observed. Due to the roll off nature of the available transducer, the area the frequencies of interest did not rise above the ambient noise level of the anechoic tank which masks any effects of scattering.

A large apparatus was constructed for dual use as an experimental platform and as an interactive public display. It has several characteristics which expand the experimental possibilities. The larger size and square sides allow for high speed photographic work as well as allowing for the use of larger transducers. As a public display the apparatus will provide interactive education as well as visual impact.

B. FUTURE WORK

1. Formation of a Toroidal Bubble

Using the apparatus built by Hobbs, it is impossible to develop good high speed photography to capture the formation and development of a toroidal bubble in the initial stages. The circular nature of the tank produces false

reflections and distortions in the photographic images. The large apparatus is constructed out of flat sides and should eliminate these photographic problems. The acoustic emission experiment could be repeated in the large apparatus while each air burst is recorded through the use a high speed film. The photographic images could then be correlated to the time series emission plots. This future experiment could confirm that air bursts which produce no apparent toroidal formation will in fact produce a toroidal shape that high speed photography can confirm what is not visible to the naked eye. High speed photography could also determine what structural modes are creating the beating effect observed in some smooth toroidal bubble examples.

2. Scattering Experiment

The scattering experiment can be improved with the use of an acoustic transducer with a resonance frequency between 400-600 Hz. Also, the anechoic foam used for the side walls of the tank begins to lose anechoic properties below 10 kHz so future work could repeat the experiment in an improved tank or another facility which has better low frequency anechoic properties .

3. Modifications to the Large Apparatus

As stated in Sec. A, the large apparatus also serves as quality hands-on public display for the physics department hallway. Improvements to the system will increase the public interaction with the apparatus. Already included in the apparatus is a touch pressure button for external triggering the solenoid. Future areas of development for greater public interaction are an accessible pressure regulator for changing bubble sizes. Such a regulator would have mechanical limits to prevent over or under pressurization and a pin to prevent the removal of the controlling knob. One possible way to avoid this problem is with a dedicated digital pressure controller.

In the current configuration, the large apparatus will make use of the HP33120A function generator and a Techron 5507 power amplifier to develop the pulse to open the solenoid valve. A future project could construct a dedicated function generator from integrated circuits and replace the amplifier with a less expensive car stereo model. These specially constructed systems circuits could be displayed behind the clear acrylic cover in the stand.

4. Scaling the Toroidal Bubbles

The potential exists for future development of a toroidal bubble apparatus which scales down the size of the toroidal bubble. Such small bubbles would have resonant frequencies in the kHz range and have several potential future applications for use by the Navy, for example: ship self noise level reduction and improved acoustic decoys.

5. Thunderstorm Air Studies

Though column vortex in a thunderstorm is made up of air, the updrafts and downdrafts are made up of different densities due to temperature and water state. It is possible that a thunderstorm which supports a column vortex could have an acoustic emission frequency structure which could similarly be classified into a turbulent or laminar flow as predictive element to tornado formation. Much work would have to be done to establish if any emissions exits and to correlate any acoustic emissions to thunderstorm development.

Ambient 1 (n=20)	
Mean	2.8375
Standard Deviation	0.762039
Median	2.665
Mode	2.17
Standard Error	0.170397
Sample Variance	0.580704
Minimum	2.17
Maximum	5.57
Sum	56.75
Count	20
Confidence Level (95%)	0.356645

Table AP.1. Ambient noise descriptive statistics run one (n=20)

Ambient 2 (n=20)	
Mean	2.769
Standard Deviation	0.432701
Median	2.7
Mode	2.79
Standard Error	0.096755
Sample Variance	0.187231
Minimum	2.17
Maximum	4.23
Sum	55.38
Count	20
Confidence Level (95%)	0.202511

Table AP.2. Ambient noise descriptive statistics run two (n=20)

Ambient 3 (n=20)	
Mean	2.7415
Standard Deviation	0.35491
Median	2.77
Mode	2.83
Standard Error	0.07936
Sample Variance	0.125961
Minimum	2.1
Maximum	3.33
Sum	54.83
Count	20
Confidence Level (95%)	0.166103

Table AP.3. Ambient noise descriptive statistics run three (n=20)

Ambient Total (n=60)	
Mean	2.782667
Standard Deviation	0.538072
Median	2.7
Mode	2.6
Standard Error	0.069465
Sample Variance	0.289522
Minimum	2.1
Maximum	5.57
Sum	166.96
Count	60
Confidence Level (95%)	0.138999

Table AP.4. Ambient noise descriptive statistics run combined total (n=60)

Band Passed Noise Run 1 (n=20)	
Mean	2.8705
Standard Deviation	0.908489
Median	2.76
Mode	2.21
Standard Error	.203144
Sample Variance	0.825352
Minimum	2.21
Maximum	6.47
Sum	57.41
Count	20
Confidence Level (95%)	0.425186

Table AP.5. Band-passed noise descriptive statistics run one (n=20)

Band Passed Noise Run 2 (n=20)	
Mean	2.6545
Standard Deviation	0.282796
Median	2.625
Mode	2.69
Standard Error	0.063235
Sample Variance	0.079973
Minimum	2.15
Maximum	3.32
Sum	53.09
Count	20
Confidence Level (95%)	0.132352

Table AP.6. Band-passed noise descriptive statistics run two (n=20)

Band Passed Noise Run 3 (n=20)	
Mean	2.7135
Standard Deviation	0.336863
Median	2.685
Mode	2.45
Standard Error	0.075325
Sample Variance	0.13477
Minimum	2.26
Maximum	3.47
Sum	54.27
Count	20
Confidence Level (95%)	0.157657

Table AP.7. Band-passed noise descriptive statistics run three (n=20)

Band Passed Total (n=60)	
Mean	2.746167
Standard Deviation	0.58012
Median	2.67
Mode	2.77
Standard Error	0.074893
Sample Variance	.336539
Minimum	2.15
Maximum	6.47
Sum	164.77
Count	20
Confidence Level (95%)	0.149861

Table AP.8. Band-passed noise descriptive statistics combined total (n=60)

LIST OF REFERENCES

Acheson, D. J., *Elementary Fluid Dynamics* (Oxford, New York, 1990), pp. 168-169.

Batchelor, G. K., *An Introduction to Fluid Dynamics* (Cambridge, New York, 1967), pp. 522-526.

Blake, John R., Keen, Giles S., and Tong, Robert P., and Miles Wilson, "Acoustic cavitation: The fluid dynamics of non-spherical bubbles," Phil. Trans. R. Soc. Lond. A **357**, 251-267 (1999).

Chen, Li, Garimella, Suresh V., Reizes, John A., and Leonardi, Eddie, "The development of a bubble rising in a viscous liquid," J. Fluid Mech. **387**, 61-96 (1999), and references therein.

Faber, T. E., *Fluid Dynamics for Physicists* (Cambridge, New York, 1995), pp. 415-423.

Fitzgerald, Richard, "An optical spoon stirs up vortices in a Bose-Einstein condensate," Phys. Today, August 2000, pp. 19-21.

Hobbs, Allen, *Construction and Quantification of a Toroidal Bubble Apparatus* (M.S. thesis, Department of Physics, Naval Postgraduate School), September 2000.

Lamb, Horace, *Hydrodynamics*, 6th ed., 1932 (reprinted by Cambridge University Press, New York, 1997), ch. VII.

Larraza, A. and Tucholski, E., "Acoustic Enstein-Hopf Drag on a Bubble," Physical Review Letters **84**, 2378-2380 (2000).

Lemerande, T., LT USN, "Dual Tri-Laminar Flexural Disk Projector,"(Department of Physics, Naval Postgraduate School), student report for prof Hofler's PH4454 class December 2001.

Lundgren, T .S., Mansour, N. N., "Vortex ring bubbles," J. Fluid Mech. **224**, 177-196 (1991).

Marten, Ken, Shariff, Karim, Psarakos, Suchi, and White, Don J., "Ring bubbles of dolphins," Sci. Am., August 1996, pp. 83-87.

Metzer, Stephen M., Carr, James R., Johnson, Jeffrey R., Parke, Timothy J r, and Lemmon, Mark T., "Techniques for identifying dust devils in Mars Pathfinder images," IEEE Trans. on Geosci. and Rem. Sens. **38**, 870-876 (2000).

Pedley, T. J., “The toroidal bubble,” J. Fluid Mech. **32**, part 1, 97-112 (1968).

Putterman, Seth J., *Superfluid Hydrodynamics* (North-Holland/American Elsevier, New York, 1974), pp. 7-9, 32-34, 72-78, ch. II, 163-177, 181-194, 251-262, 309-330, app. V.

Rief, F., “Quantized vortex rings in superfluid helium,” Sci. Am., Dec. 1964, pp. 116-122.

Semper, Robert J., “Toroidal bubbles,” Nature **356**, 390 (1992).

Shankar, P. N., Kumar, Manoj, “Toroidal vortex rings,” Cur. Sci. **66**, 151-153 (1995).

Sussman, Mark and Smereka, Peter, “Axisymmetric free boundary problems,” J. Fluid Mech. 341, 269-294 (1997).

Turner J. S., “Buoyant vortex rings,” Proc. Roy. Soc. A **239**, 61-75 (1957).

Walters, J. K. and Davidson, J. F., “The initial motion of a gas bubble formed in an inviscid liquid. Part 2: The three-dimensional bubble and the toroidal bubble,” J. Fluid Mech. **17**, 321-336 (1963).

INITIAL DISTRIBUTION LIST

1. Defense Technical Information Center
   Ft. Belvoir, Virginia

2. Dudley Knox Library
   Naval Postgraduate School
   Monterey, California

3. Professor Bruce C. Denardo, Code PH/Db
   Department of Physics
   Naval Postgraduate School
   Monterey, California

4. Professor Ronald Brown, Code PH/Br
   Department of Physics
   Naval Postgraduate School
   Monterey, California

5. Undersea Warfar Programs Office, Code 35
   Naval Postgraduate School
   Monterey, California

6. Ashley M. Harris
   Vian, Oklahoma